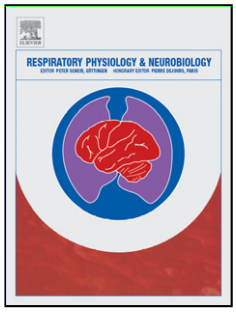

Title: Metabonomic profiling of chronic intermittent hypoxia in a mouse model

Authors: Stéphanie Conotte, Alexandra Tassin, Raphaël Conotte, Jean-Marie Colet, Karim Zouaoui Boudjeltia, Alexandre Legrand

PII: S1569-9048(17)30218-5
DOI: https://doi.org/10.1016/j.resp.2018.02.015
Reference: RESPNB 2935

To appear in: *Respiratory Physiology & Neurobiology*

Received date: 18-7-2017
Revised date: 26-1-2018
Accepted date: 27-2-2018

Please cite this article as: Conotte, Stéphanie, Tassin, Alexandra, Conotte, Raphaël, Colet, Jean-Marie, Boudjeltia, Karim Zouaoui, Legrand, Alexandre, Metabonomic profiling of chronic intermittent hypoxia in a mouse model.Respiratory Physiology and Neurobiology https://doi.org/10.1016/j.resp.2018.02.015

Metabonomic profiling of chronic intermittent hypoxia in a mouse model

Stéphanie Conotte[a], Alexandra Tassin[a], Raphaël Conotte[b], Jean-Marie Colet[b], Karim Zouaoui Boudjeltia[c], Alexandre Legrand[a*]

Laboratory of Respiratory Physiology, Pathophysiology and Rehabilitation [a], *Laboratory of Human Biology and Toxicology* [b], *Research Institute for Health Sciences and Technology, University of Mons, Mons, Belgium; Laboratory of Experimental Medicine (ULB 222 Unit), Medicine Faculty, Université Libre de Bruxelles, CHU de Charleroi, Belgium* [c].

*Author to whom reprint requests should be addressed. Email: alexandre.legrand@umons.ac.be

There is no conflict of interest regarding the publication of this paper.

Address for correspondence:
Prof. A. Legrand
Lab. Respiratory Physiology and Rehabilitation, University of Mons
Avenue du Champ de Mars, 6
B-7000 Mons, Belgium
Tel : 32-65-373554; e-mail : alexandre.legrand@umons.ac.be

Highlights

- This first metabonomic urinary profiling in a Chronic intermittent hypoxia (ChIH) murine model allows a better understanding of systemic effects of this key component of obstructive sleep apnea (OSA) pathophysiology.
- ChIH, per se, is sufficient to induce an oxidative stress (OS) imbalance *in vivo*, followed by a modulation of antioxidant defence over time.
- Energy metabolism is modified by ChIH, with a switch towards anaerobic pathways, likely partly mediated by a transient activation of HIF1α.
- Signs of a higher vitamin B3 production could be indicative of an increased need of coenzymes NAD^+ and $NADP^+$ regeneration upon exposure to ChIH.
- Hipurrate, a marker of liver function, is modulated after a long-term exposure to ChIH.
- Trimethylamine N oxide (TMAO) and allantoïn could constitute promising biomarkers in the context of cardiovascular risk and OS associated to OSA.

Abstract :

Chronic intermittent hypoxia (ChIH) is a dominant feature of obstructive sleep apnoea (OSA) and is associated to metabolic alterations and oxidative stress (OS). Although management of OSA is well established, the research of new biomarkers that are independent of confounding factors remains necessary to improve the early detection of comorbidity and therapeutic follow-up.
In this study, the urinary metabonomic profile associated to intermittent hypoxia was evaluated in a mouse model.
When exposed to intermittent hypoxia, animals showed a significant alteration in energy metabolism towards anaerobic pathways and signs of OS imbalance. A compensatory response was observed over time. Our data also indicates an excess production of vitamin B3, liver function modulations and a stimulation of creatine synthesis which could be used to evaluate the ChIH repercussions. As well, TMAO and allantoin could constitute interesting biomarker candidates, respectively in the context of cardiovascular risk and OS associated to OSA.

Abbreviations:

AUC : area under the curve
ChIH : chronic intermittent hypoxia
CPAP : continuous positive airway pressure
FID : free induction decays
FIO_2 : fraction of inspired oxygen
FMO3 : flavin-containing monooxygenase-3
GAMT : guanidinoacetate methyltransferase
GLUT : glucose transporter
H_2O_2 : hydrogen peroxide
HIF1 : hypoxia inducible factor 1
HRE : hypoxia responsive element
IH : intermittent hypoxia
NAFLD : nonalcoholic fatty liver disease
^{1}H-NMR : proton nuclear magnetic resonance
NRF2 : NF-E2 related factor 2
OS : oxidative stress
OSA : obstructive sleep apnoea
PDK1 : pyruvate dehydrogenase kinase 1
PLS-DA : partial least squares discriminant analysis
ROS : reactive oxygen species
SOD : superoxide dismutase
TCA : tricarboxylic acid
TMA : trimethylamine
TMAO : trimethylamine N oxide
UA : upper airway

Key Words: obstructive sleep apnoea, intermittent hypoxia, metabonomic, oxidative stress.

1. Introduction

Obstructive sleep apnoea (OSA) is one of the most frequent sleeping disorder and is identified by the National Commission on Sleep Disorders Research as being a major public health problem in particular from resulting cardiovascular comorbidities (Destors et al., 2014; Sánchez-de-la-Torre et al., 2013). This pathology affects at least 2 – 4% of men and 1 – 2% of women over 50 years (Angelico et al., 2010; Avellar et al., 2015; Dempsey et al., 2010) but the prevalence of OSA in case of obesity exceeds 50% (Drager et al., 2010). This syndrome is characterized by episodes of upper airway (UA) obstruction caused by an inability of the UA muscles to maintain airway patency during sleep (Carrera et al., 1999; Dempsey et al., 2010; McGuire et al., 2002).

Each apnoea episode is combined to a decreased haemoglobin oxygen saturation and recurrent arousal inducing abrupt re-oxygenation. Chronic intermittent hypoxia (ChIH) is a typical feature of OSA which is known to lead to an increased inflammatory response, an endothelial dysfunction and oxidative stress (OS) (Chiang, 2006; Lavie, 2003). The hypoxic stress is frequently associated to a metabolic dysfunction characterized by an insulin resistance, type II diabetes or metabolic syndrome (Chiang, 2006), in addition to cardiovascular morbidity. The lipid metabolism is also affected and dyslipidaemia and lipid peroxidation are observed in human and animal studies (Jun and Polotsky, 2009, 2007). However, metabolic disruption in favour of a decrease in either glycolytic or oxidative metabolism both exists in OSA patients (Vanuxem et al., 1997) but these changes seem to be dependent on exposure and severity of hypoxia (Clanton and Klawitter, 2001).

ChIH induces a compensatory response through the activation of different transcription factors, to counteract the detrimental impact of hypoxia. Among these, HIF1 (Hypoxia Inducible Factor 1) is known to regulate the expression of numerous genes involved, inter alia, in glucose metabolism in favour of anaerobic pathways (Gothié and Pouysségur, 2002; Maes et al., 2012; Van Thienen et al., 2017).

Diagnosis and treatment of OSA are well codified. Currently, the gold standard for OSA diagnosis is the polysomnography. However, this diagnosis tool is time consuming and some important limitations exist such as the cost and a reduced widespread availability (De Luca Canto et al., 2015). Due to the lack of importance granted to excessive snoring and daytime sleepiness, only 15% of people with suggestive symptoms of OSA benefit from polysomnography in France. This percentage rises to 26-28% in patients with other risk factors such as hypertension, obesity and diabetes (Fuhrman et al., 2012). These data are notably consistent with a study conducted in 2007 in the United States, where 19% of symptomatic patients had benefited from polysomnography (Thornton et al., 2010). As regards the treatment, continuous positive airway pressure (CPAP) is considered to be an effective treatment for OSA. However, mild OSA is often not eligible for this treatment, even if mild OSA is associated to an increased risk of cardiovascular and metabolic comorbidity (Brown, 2007; Hla et al., 2015).A poor compliance to this treatment is also not unusual and some patients continue to have residual sleepiness in spite of therapy (Chiang, 2006; De Luca Canto et al., 2015; Dempsey et al., 2010; Montesi et al., 2012; Somers et al., 2008). Unfortunately, inadequately treated patients conserve a higher risk of comorbidity (Campos-Rodriguez et al., 2014).

For all these reasons, scientists are looking for alternative diagnostic and follow-up testing. To this aim, a special interest has centred around potential OSA biomarkers (De Luca Canto et al., 2015). Inflammatory (TNFα and IL6), metabolic (glucose regulation) and OS (8 isoprostane and NO) markers as well as hypertension, are frequently evaluated in this pathology. Although these potential biomarkers have proved to be promising to improve the diagnostic and the treatment of

OSA, these are not considered to be ideal because of confounding factors (such as obesity) which might interfere with data interpretation (De Luca Canto et al., 2015; Jun and Polotsky, 2009; Montesi et al., 2012). To limit the impact of these confounding factors in the understanding of pathophysiological mechanisms involved in OSA, reductionist models can be used to better characterize the ChIH component of the disease (Chopra et al., 2016). In the literature, multiple protocols have been reported to evaluate this component. The number and length of intermittent hypoxia (IH) cycles, the total period of exposure of these cycles and the depth and duration of hypoxia are some of the major differences between reported methodologies (Béguin et al., 2005; Ishii et al., 2010; McGuire et al., 2002). In our laboratory, ChIH exposure is performed by using a device allowing to expose mice to rapid variation of oxygenation mimicking the pattern observed in severe OSA (in terms of cycles of hypoxia-reoxygenation and severity of desaturation) (Chodzyński et al., 2013). Moreover, contrary to other models where submission to the same air-conditions is not guaranteed (Béguin et al., 2005; Ishii et al., 2010; McGuire et al., 2002), our device allows to submit all mice to similar standardized and controlled air-flow conditions (Chodzyński et al., 2013).

Recently, metabonomics, a new complementary tool to genomics and proteomics, appears as one of the most powerful predictive technique to determine the systemic biochemical profiling by analysing tissues and biofluids such as plasma or urine (Nicholson et al., 2002; Shockcor and Holmes, 2002). This technique is based on the qualitative and quantitative measurement of multiparameter metabolic response of living systems in response to physiological stimuli or genetics modifications. The metabolome is constituted by all small-molecular-weight compounds (< 1500 Da) contributing to intermediate metabolism (Dunn et al., 2005; Lindon and Nicholson, 2008). In the present study, proton nuclear magnetic resonance (^{1}H-NMR) spectroscopy was used. This non-destructive and non-invasive technique provides detailed information on molecular structure and allows the detection of a wide range of metabolites simultaneously (Beckonert et al., 2007; Lindon et al., 2000).

To date, only few small sample-size metabonomic profiles have been reported for OSA (Ferrarini et al., 2013; Ząbek et al., 2015) and the temporal evolution of these profiles remains essentially unknown. Very recently, one study determined a urinary metabolomic profiling in OSA and simple snorers patients. Although these metabolite signatures could potentially serve as an alternative diagnostic method to polysomnography, this pilot exploratory study was performed on a relatively small sample size. Moreover, it seems necessary to clarify in what extend any confounding factors and coexisting diseases may have an impact on metabolomic results. Finally, there are no data available regarding the effect of CPAP treatment or the impact of isolated IH on metabolomic profiling (Xu et al., 2016). In addition, there is no available data concerning the temporal evolution of this metabolomic pattern during IH exposure.

The present study aimed at better understanding the metabolic alterations specifically induced by ChIH. To this aim, .

we investigated, in our reductionist ChIH murine model (Chodzyński et al., 2013), the urinary metabonomic profile after either a short or a long exposure to ChIH to evaluate modulations over time. Hypotheses regarding biochemical pathways probably involved in the metabolic signature were then verified. This approach allowed us to identify urinary markers potentially useful for the diagnosis and follow-up of patients with OSA.

2. Methods

2.1. Ethical approval

All procedures met the standards of the national Belgian requirements regarding animal care and were carried out in accordance with the Animal Ethics and Welfare Committee of the University of Mons. Male C57BL6J mice (weighing 26 ± 2.4 g) were obtained from an internal breeding animal facility from the University of Mons (accreditation number LA1500022).

2.2. Animals

Except during the experimental periods, mice were housed at 35-40% relative humidity, a temperature of 20-23°C under a 12:12 (light:dark) photoperiod and with an ad libitum access to food (RN-01-20K12, Carfil quality) and water. At the age of 9 weeks, animals were randomized in control (sham) or intermittent hypoxia (ChIH) groups. Food intake and body weight were measured once a day during the first 4 days and then once a week during the following 5-week of the protocol. At the end of experimentation, animals were sacrificed by an intraperitoneal injection of Nembutal ® (60 mg/kg, Ceva santé animal) and exsanguination by vena cava puncture.

2.3. Design of study

During the protocol, mice were placed in a validated device allowing a controlled exposure to IH in individual chambers as described in our previous publication (Chodzyński et al., 2013). Briefly, this system was constituted to a nitrogen and an air compressor connected respectively to a tank. The flow lines were controlled by two analogical valves in order to obtain the required oxygen concentration. Two digital valves allowed modulating the flow to obtain very fast variations of ambient fraction of inspired oxygen (FIO_2) in the exposition chamber. An oxygen captor was placed at the end of circuitry to verify the composition of gas mixture in real time. For the ChIH group, cycles of 30 s to the FIO_2 of 6 ± 1 % - 30 s to the FIO_2 of 21 ± 1% were performed. These cycles were repeated 8h/d for 35 days. For the sham group, air was distributed during the same time in identical chambers. A schematic representation of the timeline is illustrated in **Figure A** and the number of animals per group and time points is indicated in the legend**.**

2.4. Metabonomic analyse

14 animals were randomly affected to either ChIH or Sham group, and followed from days 0 to 35. At different time points (day 0 (= pre-test urine), 1, 2, 3, 4, 7, 14, 21, 28 and 35, figure A3), animals were placed directly after IH or normoxic exposure in metabolic cages, and samples of urine were collected for 16h. As biofluids were very prone to microbiological contamination, samples were collected into tubes containing 500 µl of NaN_3 (0.1 M) over ice. 200 µl of urine were then added to 200 µl of distilled water and 200 µl of phosphate buffer (Na_2HPO_4 0.2 M and NaH_2PO_4 0.04 M in a mix H_2O/D_2O (80:20) ; pH 7.4). The solution was then centrifuged at 13000 g for 10 minutes at room temperature (RT). 50 µl of the solution containing 3-(trimethylsilyl) propionic-2,2,3,3-d4 acid (TSP) (0.1 mM) and D_2O were added to the supernatant. 500 µl of sample were finally placed into 5 mm NMR tube for analysis. All the analyses were recorded at 297°K using a Bruker Avance 500 spectrometer at 500 MHz with 5 mm BBI PROB for proton observation (General, Organic and Biomedical Chemistry Department, UMONS, Mons, Belgium). One-dimensional spectrum was acquired using a NOESYPRESAT-1d pulse sequence. For each sample, 64 free induction decays (FIDs) with 54832 data point per FID were collected using a spectral width of 10330.5 Hz, an acquisition time of 2.65s and a pulse recycle delay of 3s. The FID was Fourier transformed and a line broadening of 0.3 Hz was applied. The spectra were corrected and calibrated against TSP

arbitrarily placed at 0.00 ppm using 5.3.0-4536 MestReNova software (MestreLab Research S.L., Santiago de Compostela, Spain).
Spectral data were then converted into numerical data. To this goal, the spectral regions (from 0.08 ppm to 10.00 pm) were reduced to 248 regions of 0.04 ppm width each and next integrated. Regions corresponding to the residual water signal (from 4.50 ppm to 5.00 ppm) and the daily urea variation (from 5.50 ppm to 6.00 ppm) were then excluded. Each integrated sub-region was normalized to the total spectrum area. The final data set was imported into SIMCA-P+12.0 software (Umetrics, Umea, Sweden). After mean-centering of the data with Pareto scaling, a partial least squares discriminant analysis (PLS-DA) was performed. This analysis was carried out to discriminate the metabolic patterns between treated and sham mice and also between hypoxic animals to observe differences over time. A scores scatter plot was then realized to evaluate relationships between observations and a loadings scatter plot to determine the spectral area differing between the groups. The quality and reliability of the models were assessed by the R^2 and Q^2 parameters. The goodness of fit parameter R^2 represents the explained variation in the data and the goodness of prediction parameter Q^2 uses cross-validation to estimate the predictive ability of the model. A CV-ANOVA test was performed to evaluate statistical significance (Eriksson et al., 2008). To further validate the established model, a random permutation test with 50 permutations was performed with PLS-DA. Metabolite identification was then realized with an identification table on spectral area having a VIP (variable important in projection) > 0.7.

2.5. Blood and tissue sampling and analyse.

76 additional animals were allocated to ChIH or Sham group and sacrificed at different time-points for blood and tissue sampling.

2.5.1. Haematocrit measurement

To confirm that exposure to ChIH (FIO2 21% - 6%, 30s – 30s, 8h/day) reproduced OSA characteristics, we first assessed the emergence of a polycythaemia at different time-points (days 1, 3, 8, 14, 21, 28 and 35; **Figure A1**). Haematocrit measurement was immediately realized after the 8-hours IH or sham exposure.

2.5.2. Glucose Tolerance Test

Because ChIH is known to stimulate anaerobic glycolysis pathway by a series of adaptive responses, which prone to modify glucose tolerance (Goda and Kanai, 2012; Toffoli et al., 2007; Yuan et al., 2008), a glucose tolerance test was performed directly after the 8 hours of treatment (corresponding to fasting) at different time points (day 0, 1, 3, 7, 14, 21, 28 and 34, **Figure A2**). To this aim, mice received an intraperitoneal glucose injection (2g/ kg body weight of D-glucose (Roth, Karlsruhe, Germany). Glycemia was measured before and 30, 60 and 120 minutes after injection by using glucometer (OneTouch® Vita™, LifeScan, Inc., USA). The area under the curve (AUC) of glycemia was then calculated.

2.5.3. HIF1α activation

Because HIF1α is known as a key mediator of the adaptive response to hypoxia, its activation was evaluated by a relative quantification of its nuclear protein abundance. To this aim, animals were sacrificed at time points (Days 1 and 35) directly after the 8 hours of IH. A liver sample was harvested, placed in liquid nitrogen and kept at -80°C.

To evaluate HIF1α activation, nuclear extracts were prepared from liver tissue by using the NE-PER™ (Nuclear and Cytoplasmic Extraction Reagent Kit, 78833, ThermoFisher Schientific) with protease and phosphatase inhibitor cocktail (Sigma-Aldrich and VWR, respectively), according to manufacturer's instructions. 150 µg of nuclear extracts were then separated by an 8% SDS-PAGE for 2h20 at 100V and transferred to a nitrocellulose membrane (GE Healthcare). The membrane was then cut in 2 parts at around the 50kDa molecular weight marker (Biorad).
On the upper part, after blocking with 5% non-fat dry milk-TBS for 1h30 at RT, membranes were incubated overnight at 4°C with a rabbit pAb directed against HIF-1α (1/500, NB100-479, Novus Biologicals). After deionised rinsing, membranes were then incubated with a HRP-conjugated secondary antibody (1/5000, NA934V, GE Healthcare) for 1h at RT. The revelation step was performed using SuperSignal™ West Femto Maximum Sensitivity Substrate (34095, ThermoFisher Scientific).
On the lower part, after blocking with 5% BSA TBS-T for 1h at RT, membranes were incubated with a Rb mAb anti-RPLP0 (1/1000, ab192866, Abcam). After TBS-T rinsing, membranes were then incubated with a HRP-conjugated secondary antibody (1/5000, NA934V, GE Healthcare) for 1h at RT. The revelation step was performed using ECL™ Western Blotting Reagents (GE Healthcare). The immunoreactive bands were then submitted to a densitometric analysis using the Image J software and data normalized to RPLP0 bands.

2.5.4. Creatine synthesis assessment

ChIH modulating energy metabolism towards anaerobic pathways, we decided to investigate the last step of creatine synthesis by a relative quantification of GuanidinoAcetate MethylTransferase (GAMT) protein abundance by western blot. During protocol adjustments, different bands, which potentially corresponded to dimeric or trimeric forms, were immunodetected in liver extracts. Therefore, the relative amounts of these GAMT forms were first determined on liver extracts obtained by lysis in KPO_4 buffer (1M K_2HPO_4, 1M KH_2PO_4 and protease inhibitor cocktail (Sigma-Aldrich)) using a non-reducing SDS-PAGE. This analysis was also realized in strong reducing conditions by using liver extracts realized in urea buffer (50mM Tris, 5M urea and 0.5% β-mercaptoethanol, DTT and protease inhibitor cocktail (Sigma Aldrich)).
In both cases, 30 µg of total protein extract were separated by a 12% gel (1h45, 100V) and transferred to nitrocellulose membrane (GE Healthcare). After blocking with 0.2% non-fat dry milk TBS-T for 1h at RT, membranes were probed with a primary Rb pAb anti-GAMT antibody (1/4000, 10880-1-AP, bio-connect) and then incubated with a HRP-conjugated secondary antibody (1/5000, NA934V, GE Healthcare) for 1h at RT. The revelation step was performed using ECL™ Western Blotting Reagents (GE Healthcare). The immunoreactive bands were then submitted to a densitometric analysis using the Image J software and data normalized to RPLP0 bands.

2.6. Statistics

For each analyse, normality and equal variance tests were assessed using respectively Shapiro-Wilk test and Levene median test. All data were represented as mean ± sem or boxplot (25^{th} and 75^{th} percentile) for parametric or non-parametric statistical test, respectively. The mean values of haematocrit, body weight and food intake were calculated and assessed using a One Way ANOVA (haematocrit) or Two Way ANOVA for Repeated Measure, followed by a Student-Newman-Keuls test. Median, 25^{th} and 75^{th} percentile were calculated for HIF1 activation measurement and glucose

tolerance test results. Median of each analysis were then compared between sham and hypoxic mice by using an Analysis of Variance on Ranks (Dunn's Method). A student's unpaired t-test was used to determine the statistical significance of total GAMT expression, whereas a Chi square was performed for GAMT distribution. Differences were considered statistically significant for $p < 0.05$.

3. Results

Chronic intermittent exposure to hypoxia was well tolerated. Besides a slight decrease of body weight at the beginning of the protocol, body weight (**Appendix A.1**, $p = 0.121$) and food intake (**Appendix A.2**, $p = 0.397$) were not significantly affected.

3.1. Metabolic changes between hypoxic and sham animals

To investigate major differences in the urine metabolite composition of sham and ChIH mice, multivariate data analysis was built using ^{1}H NMR data. The PLS-DA ($R^2Xcum = 0.377$; $Q^2cum = 0.366$) (**Figure B.1**) showed a significant separation between sham and ChIH mice ($p = 5.58 \times 10^{-9}$, CV ANOVA test). The corresponding loadings plot indicated an increase in the levels of lactate (1.32 ppm doublet and 4.13 – 4.17 ppm quadruplet), hippurate (3.97 ppm, doublet and 7.79 ppm doublet), sarcosine (3.61 ppm, singlet), glycine (3.53 ppm, singlet), creatine and creatinine (3.93 ppm, singlet and 4.05 ppm, singlet), trans-aconitate (3.45 ppm, singlet), trimethylamine N oxide (3.21 ppm, singlet), allantoin (5.34 ppm and 5.42 ppm singlet) and trigonelline (4.41 ppm, singlet). In parallel, decreased levels of pyruvate (2.37 ppm, singlet), citrate (2.68 ppm, doublet), succinate (2.44 ppm, singlet), acetoacetate (2.28 ppm, singlet), methionine (2.16 ppm, singlet), isoleucine (0.92 ppm, multiplet), methylamine (2.56 and 2.60 ppm, singlet), dimethylamine (2.72 ppm, singlet), trimethylamine (2.88 ppm, singlet) and taurine (3.41 ppm, triplet) were also observed in ChIH urine (**Appendix B, Table A**). The plot presented in **Figure B.2** indicated the validity of the established PLS-DA model. **Figure C** shows representative 500 MHz ^{1}HNMR spectra of urine samples from sham and ChIH mice.

Biochemical pathways mainly deregulated in ChIH mice are summarized on **Figure I**. Globally, the increase in lactate/pyruvate ratio and trans-aconitate, together with the decreased level of citrate, succinate and acetoacetate reflected TCA cycle disruption. This disturbance indicated a switch to anaerobic metabolism in ChIH mice. Creatine, sarcosine, glycine and methionine could constitute another subgroup of metabolites, all involved in creatine synthesis.

The increased level of the oxidized form of trimethylamine (TMAO) was consistent with the lower level of methylamine, dimethylamine and trimethylamine. Alterations of other pathways could also be suspected at this stage such as oxidative stress (allantoin, taurine), vitamin B3 (trigonelline) and liver detoxification (hippurate).

3.2. Metabolic modulation over time of ChIH exposure

To better characterize metabolic changes occurring during early events and chronic alterations induced by ChIH, data collected during the first 4 days were compared to those from later time points (7 to 35 days of exposure) (**Figure D.1**). The PLS-DA performed on the ChIH data only ($R^2Xcum = 0.434$; $Q^2cum = 0.486$) showed a clear separation between the early and the late time points ($p = 9.07 \times 10^{-6}$, CV ANOVA test). The validation of the established PLS-DA model is presented on **Figure D.2**. In urine samples collected at late time point, we observed increased levels

of methylamine (2.60 ppm, singlet), dimethylamine (2.72 ppm, singlet), trimethylamine (2.88 ppm singlet), hippurate (3.97 ppm, doublet, 7.55 – 7.59 ppm doublet and 7.63 triplet), glycine (3.53 ppm singlet) and tryptophan (7.18 ppm, triplet; 7.26 and 7.3 ppm, quadruplet; 7.5 ppm, doublet; 7.71 ppm doublet), as compared to earlier samplings. The loadings plot also showed a decrease in levels of taurine (3.41 ppm, triplet), methionine (2.16 ppm, singlet), allantoin (5.42 ppm, singlet), acetoacetate (2.28 ppm, singlet), creatine / creatine phosphate or creatinine (3.01 and 3.05 ppm, singlet and 3.93 ppm singlet), sarcosine (3.61 ppm, singlet) and choline / carnitine (3.17 ppm, singlet) after prolonged exposure to ChIH (**Appendix C, Table B**). A decrease in intermediate products of tricarboxylic acid (TCA) cycle (succinate (2.40 ppm singlet), citrate (2.68 ppm doublet), trans-aconitate (3.45 ppm, singlet), cis-aconitate (3.09 ppm, singlet)) was also observed. As illustrated on **Figure I**, the increase in allantoin after a short exposure to ChIH together with the decrease in taurine level at later time point revealed a change in mechanisms of antioxidant defences over time. The increased level of tryptophan over time coupled to the higher level of trigonelline observed in 3.1, was in agreement with a perturbation of vitamin B3 metabolism. The increased level of hippurate noticed in the ChIH group was more apparent at late time point. An increase in hepatotoxic metabolite (choline and carnitine) also observed after a chronic exposure. Finally, the disturbance of energy metabolism (TCA and creatine synthesis intermediates) was detectable at late time point.

3.3. Early increase of HIF1α nuclear abundance in liver in ChIH mice.

As hypoxia is known to induce compensatory mechanisms mainly mediated through a transient activation of HIF1α, with long-term effects notably in terms of energy metabolism (Toffoli et al., 2007; Yeung et al., 2008; Yuan et al., 2008), we evaluated HIF1α activation by a relative quantification of its nuclear abundance in liver samples. The signal detected with the HIF-1 antibody shows multiple bands located around the theoretical molecular weight (110 kD). Among those, the upper ones likely correspond to various posttranslational modifications such as phosphorylated or ubiquitinated forms (Ndubuizu et al., 2009) whereas lower bands could be indicative of the presence of degradation products (**Figure E.1**). The densitometric analysis of bands located between 110 and 150 kDa showed a significant increase of HIF1α protein abundance after 1 day of ChIH as compared to sham animals, but this increment was not maintained until 35 days ($p < 0.01$, ANOVA on ranks, **Figure E.1-2**).

3.4. ChIH mice exhibit an increased haematocrit and glucose tolerance over time.

One of the adaptive responses to hypoxia mediated by HIF1α is the promotion of red blood cell formation. ChIH mice exhibited an increased haematocrit from day 8 (ChIH : 44.36 ± 1.12 % vs sham : 40.03 ± 0.98 %) up to 35 (ChIH : 45.78 ± 1.29 % vs sham : 39.64 ± 0.93 % ; $p<0.001$, One Way Anova ; **Figure F**). A reduction of the hyperglycemic response after glucose injection was also observed and indicated a better glucose uptake in ChIH mice. This improvement in glucose tolerance was present on Day 7 (blood glucose area under the curve: ChIH Day1: 19822 vs ChIH Day 7: 13507) and was maintained until Day 35 (ChIH Day 35: 11077, $p<0.001$, ANOVA on ranks). A significant decrease in AUC was also observed from Day 7 when we compared sham and ChIH data ($p<0.001$, ANOVA on ranks, **Figure G**).

3.5. ChIH induces a modification of GAMT form proportions.

Creatine being another anaerobic energy source for cells, the GAMT protein abundance was assessed as the last step of creatine synthesis. During protocol adjustments, 3 bands were observed at a molecular weight of 25 kDa, 50 and 75 kDa. Since the theoretical molecular weight of the GAMT protein was of 25kDa, a blot comparison was performed using non-denaturant and strong denaturant conditions. The results indicate that 50kD- and 75kD-bands may correspond to dimeric and trimeric forms, respectively (**Appendix D**). Consequently, a relative quantification of the total GAMT and a proportion of each form were both performed in this study. No significant difference was observed when we compared groups regarding to the total signal obtained for all GAMT forms detected upon strong denaturant conditions ($p = 0.443$, Student's unpaired t-test, **Figure H.1**). Concerning multimeric forms distribution (**Figure H.2**), the results obtained in non-denaturant conditions are indicative of a change towards an increased level of the dimeric form, as compared to sham animal ($p < 0.05$, Chi square).

4. Discussion

4.1. ChIH mice as a reductionist model of OSA

ChIH, a key component in the OSA pathophysiology, is known to induce a lot of modifications on the lipid and glucose metabolism to counteract the detrimental impact of hypoxia. However, numerous confounding factors present in OSA limit the understanding of pathological mechanisms by interfering with data interpretations. In this study, using a ^{1}H-NMR metabolic profiling approach, a characterization of our reductionist model of OSA was firstly performed to better characterize the specific impact of ChIH. Our metabonomic evaluation performed on urine samples showed a significant separation between sham and ChIH mice profiles and revealed multiple metabolic changes depending on the duration of exposure. A schematic representation of metabolite modification in ChIH was illustrated in **Figure I**. These modulations could not be attributed to any variation in body weight or food intake, those parameters being not significantly modified during the ChIH protocol.

ChIH is known to stimulate anaerobic glycolysis pathway by a series of adaptive responses, notably through HIF1α activation (Toffoli et al., 2007; Yeung et al., 2008; Yuan et al., 2008, 2005). Indeed, under hypoxic condition, the HIF1α subunit is translocated into the nucleus and forms a complex with HIF1β. This complex interacts with hypoxia responsive elements (HRE) located in the promoter regions of hypoxia-responsive genes (Gothié and Pouysségur, 2002; Maes et al., 2012; Nanduri et al., 2015). Among other effects, HIF1 pathway activation is known to stimulate tissue glucose uptake by increasing the expression and the translocation of glucose transporters (GLUT) (Goda and Kanai, 2012). Accordingly, we observed a decrease in the glycemia AUC in ChIH mice, starting on Day 7 and maintaining up to Day 35. On the other hand, these results may appear surprising given that OSA and ChIH during sleep are commonly associated with insulin resistance and diabetes (Chiang, 2006; Dempsey et al., 2010; Polak et al., 2013; Wang et al., 2015). This could reflect the direct effect of ROS production as it was described to interfere with insulin intracellular signalling pathways (Tiganis, 2011). Indeed, while insulin interact with its receptor, an H_2O_2 production occurs through NADPH oxidase, inducing notably GLUT translocation via PI3K / Akt signalling pathway or AMP/ATP ratio increment (Barbieri and Sestili, 2012; Espinosa et al., 2016; Higaki et al., 2008; Horie et al., 2008; Kwang, 2015; Mahadev et al., 2001; Mason and Wadley,

2014). However, this association is still controversial (Chopra et al., 2016; Polotsky et al., 2003; Rafacho et al., 2013), and we do not exclude the appearance of an insulin resistance in our ChIH murine model at very long-term. Future studies will be necessary to determine the exact mechanism underlying glucose tolerance changes upon ChIH.
HIF1 is also known to induce enzymes expression of the glycolytic pathway including hexokinases 1 and 3, phosphoglycerate kinase 1 and to upregulate lactate dehydrogenase A, stimulating NAD^+ regeneration, a process necessary for the maintenance of glycolysis (Goda and Kanai, 2012). The metabolic consequences of this adaptation were observed in our model by an increase of lactate/pyruvate ratio, according to Pastoris et al (1995) study realized on the gastrocnemius muscle from rats exposed to mild and severe ChIH. Moreover, decreases of citrate and succinate levels were observed in ChIH mice. Such alterations in various TCA cycle intermediates indicate that ChIH does alter oxidative phosphorylation performance. The increase of trans-aconitate, another intermediate of TCA cycle, also reflects an alteration of oxidative phosphorylation. Indeed, the presence of this metabolite indicates that cis-aconitate was not used by cells (Ganong, 2005). These signs of an altered TCA cycle seem more important after a long-term exposure to ChIH, indicating the development of a mitochondrial dysfunction over time. These results corroborate those observed by Pastoris et al on gastrocnemius muscle from rat exposed to mild or severe normobaric IH for 4 weeks. This group showed a decreased citrate concentration after mild exposure and of citrate and α-ketoglutarate levels after severe IH (Pastoris et al., 1995). These perturbations of mitochondrial metabolism could also be mediated through the activation of HIF1 signaling pathway. Indeed, this transcription factor induces expression of pyruvate dehydrogenase kinase 1 (PDK1), which inhibits pyruvate dehydrogenase. By this way, the conversion of pyruvate to acetylCoA, necessary to the function of TCA cycle, is inhibited (Goda and Kanai, 2012; Kim et al., 2006).

Our results fit with the hypothesis that TCA cycle perturbations are mediated, at least partly, through HIF1 activation upon ChIH. Accordingly, a decrease in acetoacetate, a ketone body, was observed in ChIH mice and seem to be more important following chronic exposure. It is known that acetyl-CoA produced by the beta-oxidation of fatty acids or during the conversion of pyruvate, can be metabolized to ketone bodies when acetyl-CoA is in excess (Evans et al., 2016). Therefore, the decreased acetoacetate concentration could reflect an altered beta-oxidation or a decreased pyruvate dehydrogenase activity mediated by HIF1 activation. Indeed, HIF activation, and hypoxia itself, was shown to downregulate the expression of MCAD and LCAD (medium – and long-chain acylCoA dehydrogenases), two enzymes which catalyze the first steps of fatty acid oxidation (Huang et al., 2014; Zaugg et al., 2011). Moreover, ChIH is also know to block the beta-oxidation and induce mitochondrial dysfunction through HIF1 activation (Aron-Wisnewsky et al., 2016).

In addition to switch towards anaerobic metabolism, polycythaemia (typically observed in most patients with OSA (Dempsey et al., 2010; Nasser and Rees, 1992)) appeared in our ChIH mouse model after one week of exposure and was maintain until 35 days, according to other studies (McGuire and Bradford, 1999; O'Halloran et al., 2002; Shortt et al., 2014; Skelly et al., 2012). Enhanced haematocrit is also most probably mediated by an activation of HIF1 (hypoxia inducible factor 1) transcription factor and its downstream pathways regulating compensatory mechanisms in response to hypoxia. This result confirmed the efficiency of exposure to ChIH (Haase, 2013).

Fitting with the observed metabolic perturbations and polycythaemia and to test the hypothesis of HIF1α activation, nuclear quantification of this transcription factor was performed on animals exposed to 1 and 35 days of ChIH. The nuclear quantification of HIF1α showed a significant increase in liver tissue after 1 day of exposure to IH. Accordingly, other studies also described an up-regulation of protein level HIF1α in rodent liver at different time points of exposure to IH (da Rosa et al., 2012; Li et al., 2016). In our study, a recovery to basal level of HIF1α was observed after 35 days. This result could be explained by the kinetics of HIF-1 expression, protein stabilization and nuclear translocation upon IH. Regarding this point, Stroka et al (2001) observed that 1h of continuous hypoxia (at a FIO_2 of 6%) was sufficient to increase HIF1α protein nuclear level in mice liver, with a highest expression after 1 - 2h of exposure. Thereafter, the signal declined after 3 - 4h of hypoxia (Stroka et al., 2001). Moreover, kinetics of HIF1α induction is tissue-specific. Indeed, Sacramento et al (2016) have recently described a downregulation of HIF1α expression in skeletal muscle upon ChIH (FIO_2 21%-5%, 7 min-3.5 min, 10.5 h/ day). Interestingly, this condition was associated to an insulin resistance appearing after 35 days of exposure but not present at 28 days (Sacramento et al., 2016). HIF1 activation being most probably influenced by the pattern of exposure and ROS production (Belaidi et al., 2016; Pialoux et al., 2009; Yuan et al., 2008), further analysis will be necessary to determine the exact mechanisms underlying HIF1 spatio-temporal expression after short and long-term exposure to ChIH.

4.2. Biomarker research

Although OSA diagnosis and treatment are considered to be effective, this pathology is often underdiagnosed and present some limitations such as the cost and a poor compliance with CPAP. Therefore, the identification of potential biomarkers remains necessary for OSA early diagnosis as well as to improve patient follow-up. The research of metabolic profiling on the ChIH reductionist model allow to determine ChIH specific potential biomarkers by avoiding OSA confounding factors.

Signs of adaptive mechanisms of antioxidant defenses in ChIH mice

Urinary levels of allantoin were significantly increased after a short ChIH exposure, a metabolite commonly considered as a urinary marker of OS. This oxidation product of uric acid is, therefore, a metabolic end product of xanthine metabolism (**Figure I**) (Serkova et al., 2005). In mammals, allantoin is produced either through a specific enzymatic reaction via uricase or through a simple oxido-reduction favored by many types of free radicals (Dall'Acqua et al., 2016; Hellsten et al., 1997; Mikami et al., 2000; Serkova et al., 2005). In humans, since uricase activity has not been reported to date, allantoin detection is most likely related to a non-enzymatic reaction by a direct action of reactive oxygen species (ROS). Serkova et al also observed an increased concentration of allantoin in blood and renal tissue after reperfusion of ischemic tissue in a rat kidney transplant model, known to induce a ROS production (Awad et al., 2013). The authors attribute this modulation either to an increased xanthine degradation or to a higher hydrogen peroxide (H_2O_2) production (Serkova et al., 2005).

At later time points, the decreased taurine level reinforces the hypothesis of an OS imbalance during ChIH exposure. This derivative of sulphur amino acid, found at relatively high concentrations in excitable cells and tissues exposed to high level of ROS (De Luca Canto et al., 2015; Hansen et al., 2006; Schuller-Levis and Park, 2003), contributes to a series of antioxidant defenses such as a direct

scavenging of hypochlorous acid (Schaffer et al., 2010). Increases of glutathione and glutathione peroxidase synthesis, two antioxidant defense reducing H_2O_2, were also reported to be promoted by taurine (Anand et al., 2011; Nonaka et al., 2001). Moreover, taurine is known to increase thioredoxin reductase action which allows to maintain the reduced state of the antioxidant thioredoxin (Yildirim et al., 2007) and improve zinc intracellular incorporation (Harraki et al., 1994), a metal necessary to the catalytic action of superoxide dismutase 1 (SOD1). A decrease of methionine, an essential amino acid allowing to the formation of taurine with the cysteine, is also observed. These decreases in urinary level of taurine and methionine indicate an increased consumption of this antioxidant upon ChIH.

Our results confirm the importance of IH component in OS development, as described in data relative to OSA that clearly attested the presence of OS damages in patients and categorized the pathology as an OS trouble (Barceló et al., 2006; Lavie, 2003; Lavie et al., 2004; Lavie and Lavie, 2009; Yamauchi et al., 2005). In view of these results, it seems appropriate to target biomarkers linked to OS during patient diagnosis and follow-up. Allantoin could be a good candidate since, in human, this metabolite was reported to be only present in urine following a production of ROS (Serkova et al., 2005). Although CPAP treatment is known to reduce OS (Barceló et al., 2006, 2000; Lavie et al., 2004; Minoguchi et al., 2006), we could suggest its association with an antioxidant therapy. This treatment could bring an interesting therapeutic value in view of OS repercussion in OSA pathophysiology. Antioxidant supplementation has been tested in mouse models of ChIH (Inamoto et al., 2010; Shortt et al., 2014; Skelly et al., 2012; A. L. Williams et al., 2010) and was associated to an improvement of muscular function. However, this beneficial effect was observed after 1 to 2 weeks of intermittent hypoxia exposure. The present study emphasizes the temporal evolution of the OS and an increase of the antioxidant defenses at late time-points. The real benefit of antioxidant observed in previous studies must therefore be interpreted cautiously and any further evaluation should be based on long-term studies.

Modulation of NAD+ precursors in ChIH mice

An increase in trigonelline (N-methylnicotinic acid) is observed in ChIH mice as compared to sham. This metabolite is known as the principal end-product of nicotinic acid metabolism (also called niacin, vitamin B3 or vitamin PP metabolism) (Huff and Perlzweig, 1941; Mason and Kodicek, 1970; Robinson, 2013). Consequently, the increment in trigonelline could reflect a vitamin B3 excess production inducing excretion of the excess in urines. Vitamin B3 is a precursor of coenzymes NAD^+ and $NADP^+$, which by interconversion with their reduced forms, NADH and NADPH, participate in several redox reactions and play important roles in energy metabolism (Gerhard, 1999; Sauve, 2007). Moreover, Vitamin B3 is also able to lower cholesterol levels, presumably by a reduction of VLDL production (Johnson, 2008; Pullinger et al., 2002), suggesting an anti-atherosclerotic role in hypoxic condition (Pang, 2014). An increase in tryptophan level is also observed after chronic alteration as compared to early event. This amino acid increment could corroborate the hypothesis suggesting that a more important production of vitamin B3 occurs in ChIH mice (Gerhard, 1999). However, the use of these 2 metabolites as potential biomarkers is not ideal. Indeed, vitamin B3 is a water-soluble vitamin, meaning that the organism is not able to store it. In patients, results could be distorted by a diet rich in meat and fish (Gerhard, 1999; Sauve, 2007).

Trimethylamine N oxide as a potential biomarker of OSA

The urine levels of methylamine, dimethylamine and trimethylamine were all decreased in the ChIH group as compared to sham. A concurrent increase in the level of trimethylamine N oxide (TMAO) was also observed at early and late time-points of the study. TMAO is a product derived from trimethylamine oxidation in the liver by the flavin-containing monooxygenase-3 (FMO3). These data suggest that an increased production of TMAO occurs upon ChIH condition, probably due to a stimulation of FMO3 activity. Although it is well established that TMAO plays a protective role in the maintenance of cell volume in case of osmotic or hydrostatic pressure stresses, numerous evidences indicate that TMAO could also play others functions (Lin et al., 2009; Ufnal et al., 2015). Indeed, TMAO was recently identified as a modulator of cholesterol and sterol metabolism leading, notably, to foam cells formation from macrophage, a key process in the development of atherosclerosis (Koeth et al., 2013; Randrianarisoa et al., 2016; Ufnal et al., 2015). Accordingly, numerous clinical studies also described a positive correlation between a high TMAO plasmatic level and an increased risk of cardiovascular disease (Koeth et al., 2014, 2013; Randrianarisoa et al., 2016; Sun et al., 2016; Teft et al., 2017; Wang et al., 2011). Randrianarisoa et al showed that TMAO levels was associated with an increase carotid intima-media thickness (Randrianarisoa et al., 2016). Sun et al demonstrated in culture cell that TMAO induce excessive OS (with ROS production and a decrease in SOD level), inflammatory conditions and endothelial dysfunction in HUVECs in a time and dose dependent manner (Sun et al., 2016). Moreover, recent studies suggest that FMO3 may also directly play a crucial role in the promotion of atherosclerosis and cardiovascular disease in mice (Bennett et al., 2013; Miao et al., 2015; Schugar and Brown, 2015; Shih et al., 2015; Wang et al., 2011; Warrier et al., 2015).

Nevertheless, although numerous studies suggested that the TMAO could have a role in the development of cardiovascular diseases, other studies suggested that TMAO may play a protective role by reducing deleterious effects of OS by acting as an electron acceptor (Barrett and Kwan, 1985; Lupachyk et al., 2013), neutralizing ROS leaking from the mitochondrial electron transport chain. Moreover, an increase of TMAO levels by a L-carnitine supplementation has been found to decrease markers of vascular injury and OS (ICAM-1, VCAM-1 and malonaldehyde) in patients under hemodialysis and presenting carnitine deficiency (Fukami et al., 2015). The possible pro-atherogenic or anti-atherogenic effects of TMAO and/or FMO3 in our model need to be further investigated in the aim to clarify its possible involvement in cardiovascular co-morbidities in OSA (Baguet et al., 2003; Chan and Wilcox, 2010; Dempsey et al., 2010; Destors et al., 2014; Marin et al., 2005). In any case, we envision that this metabolite could constitute a suitable candidate as a potential biomarker for OSA, whatever its role in the pathophysiology of cardiovascular risks. Indeed, patients with OSA have a higher risk to develop cardiovascular disorders such as endothelial dysfunction, atherosclerosis, cardiac hypertrophy, hypertension and dyslipidemia (Baguet et al., 2012; Dempsey et al., 2010; Destors et al., 2014). Therefore, TMAO urine level could potentially constitute a useful marker to evaluate repercussion of apnoea on the cardiovascular system. An assessment of TMAO urine level upon CPAP treatment will be necessary to examine its usefulness in the context of cardiovascular risks and OSA associations.

In our study, the increase in trimethylamine, dimethylamine and methylamine was concomitant to a decrease in choline or carnitine after chronic exposure to ChIH. The increase of these hepatotoxic metabolites is known to reduce VLDL synthesis and excretion leading to triglyceride accumulation

and *in fine* to the development of nonalcoholic fatty liver disease (NAFLD) (Leung et al., 2016; Zeisel et al., 1989). Moreover, NAFLD seems to be more aggressive in patients presenting a decrease in choline follow an increased choline metabolism in the gastrointestinal microbiota. Numerous studies show also an association between OSA severity and NAFLD progression (Arısoy et al., 2016; Aron-Wisnewsky et al., 2016; Cakmak et al., 2015; Frija-Orvoën, 2016; Mesarwi et al., 2016). Future studies will determine the possible NAFLD development upon ChIH, i.e. by a triglyceride quantification throughout exposure.

Stimulation of creatine synthesis upon ChIH

Increases in creatine, sarcosine, glycine concomitantly to a decrease in methionine were noticed in ChIH mice. We hypothesize that these metabolic variations could reflect GAMT (guanidinoacetate methyltransferase) stimulation (Hu et al., 2013; Shen et al., 2012; Zhu and Prives, 2009). GAMT intervenes in the last step of creatine synthesis from guanidoacetate. The stimulation of this enzyme induces an increased activity of methylation cycle and so reduces the level of methionine. It also stimulates the synthesis of glycine and sarcosine (also known as N-methylglycine) through the folate cycle. Arginine glycine amidinotransferase (AGAT) then transforms glycine into guanidoacetate (Dahlhoff et al., 2013; Ide et al., 2010). To verify this hypothesis, a quantification of total GAMT protein abundance in liver and proportion of GAMT forms was performed. A significant modulation of GAMT form distribution was observed after 35 days of ChIH. However, the differential level of activity of each GAMT multimeric forms remains unexplained. This stimulation is known to be mediated by p53 activation in hypoxic condition (Hu et al., 2013; Shen et al., 2012; Zhu and Prives, 2009).

Finally, the higher level of creatine in urine sample of ChIH mice may also be indicative of muscle damages upon ChIH (Ganong, 2005). This increase seems to be more important at early time points. In the context of biomarker research, the measurement of these 4 metabolites (increased in creatine, sarcosine, glycine and decreased in methionine) in urine could be particularly useful to evaluate the paraclinical repercussion of hypoxemia during the follow-up of OSA patients. However, additional research is needed to determine the exact mechanism of GAMT stimulation following ChIH exposure.

Signs of an increased phase-two detoxification in liver of ChIH mice

Hippurate is a routine clinical marker of liver function. Indeed, this metabolite is the metabolic by product of benzoic acid conjugation (Lees et al., 2013). A slow conversion of benzoic acid to hippurate suggests an impaired phase-two detoxification while a high hippurate level in urine indicates that phase-two is functioning strongly (Lavalle and Yale, 2004). In the present study, an increased hippurate level was observed and seems to develop after long-term hypoxia-reoxygenation exposure.

Regarding hippurate increase upon ChIH, two hypotheses could be suggested : **(i)** a more important activity of the gastrointestinal microbiota could be at the origin of an increase benzoic acid which could be subject to conjugation in the liver by N-acyltransferase (Moreno-Indias et al., 2015; Poroyko et al., 2016; H. R. T. Williams et al., 2010; Zhang and Davies, 2016) **(ii)** the increase of phase-two detoxification enzyme activity could reflected to an activation of NRF2 (NF-E2 related factor 2) by OS induction (Buelna-Chontal and Zazueta, 2013; Chen et al., 2015; Tkachev et al., 2011).

5. Conclusion

In conclusion, this first metabonomic urinary profiling in a ChIH murine model allows a better understanding of systemic effects of this key component of OSA pathophysiology. Indeed, our results indicate that ChIH, per se, is sufficient to recapitulate key feature of OSA : a switch towards anaerobic pathways, a polycythaemia and an increased glucose tolerance which are likely related to an early HIF1 activation. As well, our study confirm that ChIH-induced OS is a dominant feature in OSA pathophysiology. Regarding biomarker research, OS imbalance *in vivo*, followed by a modulation of antioxidant defence over time seems to be an interesting track. Among metabolites linked to OS, allantoin, a metabolite only produced by ROS action in humans, could be useful to monitor during OSA patient's treatment follow-up. It could also offer a basis for personalised treatment with antioxidant supplementation. The improvement in antioxidant defences in the time course of our study highlighted the need of chronic studies to validate the benefit of this approach. The TMAO metabolite could constitute another interesting biomarker, particularly in the context of cardiovascular risk associated to OSA. Coupled to polysomnography, TMAO urine level could constitute a non-invasive diagnostic tool and, potentially, a new indication for earlier CPAP treatment and a new tool for patient follow-up. Moreover, an increased creatine synthesis may be suspected upon ChIH, this hypothesis being reinforce through a modification of GAMT form distribution. Urine level of creatine synthesis intermediates could be interesting method to evaluate the paraclinical repercussion of apnoea but the exact mechanism of GAMT stimulation remains to be clarified.

Besides increasing our understanding of OSA pathophysiological mechanisms, this study opens new perspectives in terms of diagnosis and patient monitoring. The clinical translation of these experimental results could lead to the identification of new biomarkers of OS and cardiovascular risk, two mechanisms involved in OSA co-morbidities.

Additional information

Competing interests: The authors declare that they have no conflict of interests regarding the publication of this paper

Author contributions: SC carried out the animal experimentation, metabonomics and molecular studies, participated in the design of the study, drafted the manuscript and performed the statistical analysis. AT helped to draft the manuscript and to optimize western blot analyses. RC and JMC helped to realize metabonomic analysis and interpretation of data. KZB participated in the conception of the study and in its design and coordination. AL conceived the study, participated in its design and coordination, helped to draft the manuscript and to perform the statistical analysis.

Funding: The ISPPC (CHU Charleroi, Belgium) provides funding for the conception of device inducing intermittent hypoxia. SC held PhD fellowships from the University of Mons. The Western Blot apparatus were funded by the ABMM (Association Belge contre les Maladies neuro-Musculaires – Aide à la Recherche ASBL) and by FRMH (Fonds pour la Recherche Médicale en Hainaut).

Acknowledgements

The ISPPC (CHU Charleroi, Belgium) provides funding for the conception of device inducing intermittent hypoxia. NMR measurements were performed in the Department of General, Organic, and Biomedical Chemistry of UMONS. We thank J. Vamecq for his assistance in analyze of metabonomic results. We thank Z. Kahvecioglu, B Blairon and V. Jenart for technical assistance.

References

Anand, P., Rajakumar, D., Jeraud, M., William Fe, A.J., Balasubram, T., 2011. Effects of Taurine on Glutathione Peroxidase, Glutathione Reductase and Reduced Glutathione Levels in Rats. Pak. J. Biol. Sci. 14, 219–225. https://doi.org/10.3923/pjbs.2011.219.225

Angelico, F., del Ben, M., Augelletti, T., de Vita, R., Roma, R., Violi, F., Fabiani, M., 2010. Obstructive sleep apnoea syndrome and the metabolic syndrome in an internal medicine setting. Eur. J. Intern. Med. 21, 191–195. https://doi.org/10.1016/j.ejim.2010.03.006

Arısoy, A., Sertoğullarından, B., Ekin, S., Özgökçe, M., Bulut, M.D., Huyut, M.T., Ölmez, Ş., Turan, M., 2016. Sleep Apnea and Fatty Liver Are Coupled Via Energy Metabolism. Med. Sci. Monit. Int. Med. J. Exp. Clin. Res. 22, 908–913.

Aron-Wisnewsky, J., Clement, K., Pépin, J.-L., 2016. Nonalcoholic fatty liver disease and obstructive sleep apnea. Metabolism 65, 1124–1135. https://doi.org/10.1016/j.metabol.2016.05.004

Avellar, A.B.C.C., Carvalho, L.B.C., Prado, G.F., Prado, L.B.F., 2015. Pharmacotherapy for residual excessive sleepiness and cognition in CPAP-treated patients with obstructive sleep apnea syndrome: A systematic review and meta-analysis. Sleep Med. Rev. 30, 97–107. https://doi.org/10.1016/j.smrv.2015.10.005

Awad, E.M., Khan, S.Y., Sokolikova, B., Brunner, P.M., Olcaydu, D., Wojta, J., Breuss, J.M., Uhrin, P., 2013. Cold induces reactive oxygen species production and activation of the NF-kappa B response in endothelial cells and inflammation *in vivo*. J. Thromb. Haemost. 11, 1716–1726. https://doi.org/10.1111/jth.12357

Baguet, J.-P., Barone-Rochette, G., Tamisier, R., Levy, P., Pépin, J.-L., 2012. Mechanisms of cardiac dysfunction in obstructive sleep apnea. Nat. Rev. Cardiol. 9, 679–688. https://doi.org/10.1038/nrcardio.2012.141

Baguet, J.-P., Pépin, J.-L., Hammer, L., Lévy, P., Mallion, J.-M., 2003. [Cardiovascular consequences of obstructive sleep apnea syndrome]. Rev. Médecine Interne Fondée Par Société Natl. Francaise Médecine Interne 24, 530–537.

Barbieri, E., Sestili, P., 2012. Reactive oxygen species in skeletal muscle signaling. J. Signal Transduct. 2012, 982794. https://doi.org/10.1155/2012/982794

Barceló, A., Barbé, F., de la Peña, M., Vila, M., Pérez, G., Piérola, J., Durán, J., Agustí, A.G.N., 2006. Antioxidant status in patients with sleep apnoea and impact of continuous positive airway pressure treatment. Eur. Respir. J. 27, 756–760. https://doi.org/10.1183/09031936.06.00067605

Barceló, A., Miralles, C., Barbé, F., Vila, M., Pons, S., Agustí, A.G., 2000. Abnormal lipid peroxidation in patients with sleep apnoea. Eur. Respir. J. 16, 644–647.

Barrett, E.L., Kwan, H.S., 1985. Bacterial Reduction of Trimethylamine Oxide. Annu. Rev. Microbiol. 39, 131–149. https://doi.org/10.1146/annurev.mi.39.100185.001023

Beckonert, O., Keun, H.C., Ebbels, T.M.D., Bundy, J., Holmes, E., Lindon, J.C., Nicholson, J.K., 2007. Metabolic profiling, metabolomic and metabonomic procedures for NMR spectroscopy of urine, plasma, serum and tissue extracts. Nat. Protoc. 2, 2692–2703. https://doi.org/10.1038/nprot.2007.376

Béguin, P.C., Joyeux-Faure, M., Godin-Ribuot, D., Lévy, P., Ribuot, C., 2005. Acute intermittent hypoxia improves rat myocardium tolerance to ischemia. J. Appl. Physiol. Bethesda Md 1985 99, 1064–1069. https://doi.org/10.1152/japplphysiol.00056.2005

Belaidi, E., Thomas, A., Bourdier, G., Moulin, S., Lemarié, E., Levy, P., Pépin, J.-L., Korichneva, I., Godin-Ribuot, D., Arnaud, C., 2016. Endoplasmic reticulum stress as a novel inducer of hypoxia inducible factor-1 activity: its role in the susceptibility to myocardial ischemia-reperfusion induced by chronic intermittent hypoxia. Int. J. Cardiol. 210, 45–53. https://doi.org/10.1016/j.ijcard.2016.02.096

Bennett, B.J., de Aguiar Vallim, T.Q., Wang, Z., Shih, D.M., Meng, Y., Gregory, J., Allayee, H., Lee, R., Graham, M., Crooke, R., Edwards, P.A., Hazen, S.L., Lusis, A.J., 2013. Trimethylamine-N-oxide, a metabolite associated with atherosclerosis, exhibits complex genetic and dietary regulation. Cell Metab. 17, 49–60. https://doi.org/10.1016/j.cmet.2012.12.011

Brown, L.K., 2007. Mild obstructive sleep apnea syndrome should be treated. Pro. J. Clin. Sleep Med. JCSM Off. Publ. Am. Acad. Sleep Med. 3, 259–262.

Buelna-Chontal, M., Zazueta, C., 2013. Redox activation of Nrf2 & NF-κB: a double end sword? Cell. Signal. 25, 2548–2557. https://doi.org/10.1016/j.cellsig.2013.08.007

Cakmak, E., Duksal, F., Altinkaya, E., Acibucu, F., Dogan, O.T., Yonem, O., Yilmaz, A., 2015. Association Between the Severity of Nocturnal Hypoxia in Obstructive Sleep Apnea and Non-Alcoholic Fatty Liver Damage. Hepat. Mon. 15, e32655. https://doi.org/10.5812/hepatmon.32655

Campos-Rodriguez, F., Martinez-Garcia, M.A., Reyes-Nuñez, N., Caballero-Martinez, I., Catalan-Serra, P., Almeida-Gonzalez, C.V., 2014. Role of sleep apnea and continuous positive airway pressure therapy in the incidence of stroke or coronary heart disease in women. Am. J. Respir. Crit. Care Med. 189, 1544–1550. https://doi.org/10.1164/rccm.201311-2012OC

Carrera, M., Barbé, F., Sauleda, J., Tomás, M., Gómez, C., Agustí, A.G., 1999. Patients with obstructive sleep apnea exhibit genioglossus dysfunction that is normalized after treatment with continuous positive airway pressure. Am. J. Respir. Crit. Care Med. 159, 1960–1966. https://doi.org/10.1164/ajrccm.159.6.9809052

Chan, K.H., Wilcox, I., 2010. Obstructive sleep apnea: novel trigger and potential therapeutic target for cardiac arrhythmias. Expert Rev. Cardiovasc. Ther. 8, 981–994. https://doi.org/10.1586/erc.10.80

Chen, B., Lu, Y., Chen, Y., Cheng, J., 2015. The role of Nrf2 in oxidative stress-induced endothelial injuries. J. Endocrinol. 225, R83-99. https://doi.org/10.1530/JOE-14-0662

Chiang, A.A., 2006. Obstructive sleep apnea and chronic intermittent hypoxia: a review. Chin. J. Physiol. 49, 234–243.

Chodzyński, K.J., Conotte, S., Vanhamme, L., Van Antwerpen, P., Kerkhofs, M., Legros, J.L., Vanhaeverbeek, M., Van Meerhaeghe, A., Coussement, G., Boudjeltia, K.Z., Legrand, A., 2013. A new device to mimic intermittent hypoxia in mice. PloS One 8, e59973. https://doi.org/10.1371/journal.pone.0059973

Chopra, S., Polotsky, V.Y., Jun, J.C., 2016. Sleep Apnea Research in Animals. Past, Present, and Future. Am. J. Respir. Cell Mol. Biol. 54, 299–305. https://doi.org/10.1165/rcmb.2015-0218TR

Clanton, T.L., Klawitter, P.F., 2001. Invited review: Adaptive responses of skeletal muscle to intermittent hypoxia: the known and the unknown. J. Appl. Physiol. Bethesda Md 1985 90, 2476–2487.

da Rosa, D.P., Forgiarini, L.F., Baronio, D., Feijó, C.A., Martinez, D., Marroni, N.P., 2012. Simulating sleep apnea by exposure to intermittent hypoxia induces inflammation in the lung and liver. Mediators Inflamm. 2012, 879419. https://doi.org/10.1155/2012/879419

Dahlhoff, C., Desmarchelier, C., Sailer, M., Fürst, R.W., Haag, A., Ulbrich, S.E., Hummel, B., Obeid, R., Geisel, J., Bader, B.L., Daniel, H., 2013. Hepatic methionine homeostasis is conserved in C57BL/6N mice on high-fat diet despite major changes in hepatic one-carbon metabolism. PloS One 8, e57387. https://doi.org/10.1371/journal.pone.0057387

Dall'Acqua, S., Stocchero, M., Boschiero, I., Schiavon, M., Golob, S., Uddin, J., Voinovich, D., Mammi, S., Schievano, E., 2016. New findings on the in vivo antioxidant activity of Curcuma longa extract by an integrated (1)H NMR and HPLC-MS metabolomic approach. Fitoterapia 109, 125–131. https://doi.org/10.1016/j.fitote.2015.12.013

De Luca Canto, G., Pachêco-Pereira, C., Aydinoz, S., Major, P.W., Flores-Mir, C., Gozal, D., 2015. Biomarkers associated with obstructive sleep apnea: A scoping review. Sleep Med. Rev. 23, 28–45. https://doi.org/10.1016/j.smrv.2014.11.004

Dempsey, J.A., Veasey, S.C., Morgan, B.J., O'Donnell, C.P., 2010. Pathophysiology of sleep apnea. Physiol. Rev. 90, 47–112. https://doi.org/10.1152/physrev.00043.2008

Destors, M., Tamisier, R., Baguet, J.-P., Levy, P., Pepin, J.-L., 2014. [Cardiovascular morbidity associated with obstructive sleep apnea syndrome]. Rev. Mal. Respir. 31, 375–385. https://doi.org/10.1016/j.rmr.2013.12.003

Drager, L.F., Jun, J.C., Polotsky, V.Y., 2010. Metabolic consequences of intermittent hypoxia: relevance to obstructive sleep apnea. Best Pract. Res. Clin. Endocrinol. Metab. 24, 843–851. https://doi.org/10.1016/j.beem.2010.08.011

Dunn, W.B., Bailey, N.J.C., Johnson, H.E., 2005. Measuring the metabolome: current analytical technologies. The Analyst 130, 606–625. https://doi.org/10.1039/b418288j

Eriksson, L., Trygg, J., Wold, S., 2008. CV-ANOVA for significance testing of PLS and OPLS® models. J. Chemom. 22, 594–600. https://doi.org/10.1002/cem.1187

Espinosa, A., Henríquez-Olguín, C., Jaimovich, E., 2016. Reactive oxygen species and calcium signals in skeletal muscle: A crosstalk involved in both normal signaling and disease. Cell Calcium 60, 172–179. https://doi.org/10.1016/j.ceca.2016.02.010

Evans, M., Cogan, K.E., Egan, B., 2016. Metabolism of ketone bodies during exercise and training: physiological basis for exogenous supplementation. J. Physiol. https://doi.org/10.1113/JP273185

Ferrarini, A., Rupérez, F.J., Erazo, M., Martínez, M.P., Villar-Álvarez, F., Peces-Barba, G., González-Mangado, N., Troncoso, M.F., Ruiz-Cabello, J., Barbas, C., 2013. Fingerprinting-based metabolomic approach with LC-MS to sleep apnea and hypopnea syndrome: a pilot study. Electrophoresis 34, 2873–2881. https://doi.org/10.1002/elps.201300081

Frija-Orvoën, E., 2016. [Obstructive sleep apnea syndrome: Metabolic complications]. Rev. Mal. Respir. 33, 474–483. https://doi.org/10.1016/j.rmr.2015.11.014

Fuhrman, C., Nguyên, X.L., Fleury, B., Boussac-Zarebska, M., Druet, C., Delmas, M.-C., 2012. Le syndrome d'apnées du sommeil en France : un syndrome fréquent et sous-diagnostiqué.

Fukami, K., Yamagishi, S., Sakai, K., Kaida, Y., Yokoro, M., Ueda, S., Wada, Y., Takeuchi, M., Shimizu, M., Yamazaki, H., Okuda, S., 2015. Oral L-carnitine supplementation increases trimethylamine-N-oxide but reduces markers of vascular injury in hemodialysis patients. J. Cardiovasc. Pharmacol. 65, 289–295. https://doi.org/10.1097/FJC.0000000000000197

Ganong, W., 2005. Physiologie médicale, De Boeck Université 2ed. ed.

Gerhard, M., 1999. Biochemical Pathways : An atlas of Biochemistry and Molecular Biology, Wiley. ed.

Goda, N., Kanai, M., 2012. Hypoxia-inducible factors and their roles in energy metabolism. Int. J. Hematol. 95, 457–463. https://doi.org/10.1007/s12185-012-1069-y

Gothié, E., Pouysségur, J., 2002. HIF-1 : régulateur central de l'hypoxie. médecine/sciences 18, 70–78. https://doi.org/10.1051/medsci/200218170

Haase, V.H., 2013. Regulation of erythropoiesis by hypoxia-inducible factors. Blood Rev. 27, 41–53. https://doi.org/10.1016/j.blre.2012.12.003

Hansen, S.H., Andersen, M.L., Birkedal, H., Cornett, C., Wibrand, F., 2006. The important role of taurine in oxidative metabolism. Adv. Exp. Med. Biol. 583, 129–135.

Harraki, B., Guiraud, P., Rochat, M.-H., Faure, H., Richard, M.-J., Fussellier, M., Favier, A., 1994. Effect of taurine, l-glutamine and l-histidine addition in an amino acid glucose solution on the cellular bioavailability of zinc. Biometals 7. https://doi.org/10.1007/BF00149554

Hellsten, Y., Tullson, P.C., Richter, E.A., Bangsbo, J., 1997. Oxidation of urate in human skeletal muscle during exercise. Free Radic. Biol. Med. 22, 169–174.

Higaki, Y., Mikami, T., Fujii, N., Hirshman, M.F., Koyama, K., Seino, T., Tanaka, K., Goodyear, L.J., 2008. Oxidative stress stimulates skeletal muscle glucose uptake through a phosphatidylinositol 3-kinase-dependent pathway. Am. J. Physiol. Endocrinol. Metab. 294, E889-897. https://doi.org/10.1152/ajpendo.00150.2007

Hla, K.M., Young, T., Hagen, E.W., Stein, J.H., Finn, L.A., Nieto, F.J., Peppard, P.E., 2015. Coronary heart disease incidence in sleep disordered breathing: the Wisconsin Sleep Cohort Study. Sleep 38, 677–684. https://doi.org/10.5665/sleep.4654

Horie, T., Ono, K., Nagao, K., Nishi, H., Kinoshita, M., Kawamura, T., Wada, H., Shimatsu, A., Kita, T., Hasegawa, K., 2008. Oxidative stress induces GLUT4 translocation by activation of PI3-K/Akt and dual AMPK kinase in cardiac myocytes. J. Cell. Physiol. 215, 733–742. https://doi.org/10.1002/jcp.21353

Hu, J., Liu, Z., Wang, X., 2013. Does TP53 mutation promote ovarian cancer metastasis to omentum by regulating lipid metabolism? Med. Hypotheses 81, 515–520. https://doi.org/10.1016/j.mehy.2013.06.009

Huang, D., Li, T., Li, X., Zhang, L., Sun, L., He, X., Zhong, X., Jia, D., Song, L., Semenza, G.L., Gao, P., Zhang, H., 2014. HIF-1-Mediated Suppression of Acyl-CoA Dehydrogenases and Fatty Acid Oxidation Is Critical for Cancer Progression. Cell Rep. 8, 1930–1942. https://doi.org/10.1016/j.celrep.2014.08.028

Huff, J.W., Perlzweig, W.A., 1941. Studies in nicotinic acid metabolism. III. metabolism and synthesis of nicotinic acid in the rat. J. Biol. Chem.

Ide, T., Chu, K., Aaronson, S.A., Lee, S.W., 2010. GAMT joins the p53 network: branching into metabolism. Cell Cycle Georget. Tex 9, 1706–1710. https://doi.org/10.4161/cc.9.9.11473

Inamoto, S., Yoshioka, T., Yamashita, C., Miyamura, M., Mori, T., Ukimura, A., Matsumoto, C., Matsumura, Y., Kitaura, Y., Hayashi, T., 2010. Pitavastatin reduces oxidative stress and attenuates intermittent hypoxia-induced left ventricular remodeling in lean mice. Hypertens. Res. Off. J. Jpn. Soc. Hypertens. 33, 579–586. https://doi.org/10.1038/hr.2010.36

Ishii, M., Iwamoto, T., Nagai, A., Sasao, G., Iwasaki, M., Kuwahira, I., 2010. Polycythemia and changes in erythropoietin concentration in rats exposed to intermittent hypoxia. Adv. Exp. Med. Biol. 662, 121–126. https://doi.org/10.1007/978-1-4419-1241-1_17

Johnson, P.R., 2008. Down-regulation of bile acid synthesis and a metabolic co-activator under hypoxic conditions – implications in obstructive sleep apnea. Med. Hypotheses 71, 530–536. https://doi.org/10.1016/j.mehy.2008.02.021

Jun, J., Polotsky, V.Y., 2009. Metabolic consequences of sleep-disordered breathing. ILAR J. 50, 289–306.

Jun, J., Polotsky, V.Y., 2007. Sleep-Disordered Breathing and Metabolic Effects: Evidence from Animal Models. Sleep Med. Clin. 2, 263–277. https://doi.org/10.1016/j.jsmc.2007.03.009

Kim, J., Tchernyshyov, I., Semenza, G.L., Dang, C.V., 2006. HIF-1-mediated expression of pyruvate dehydrogenase kinase: a metabolic switch required for cellular adaptation to hypoxia. Cell Metab. 3, 177–185. https://doi.org/10.1016/j.cmet.2006.02.002

Koeth, R.A., Levison, B.S., Culley, M.K., Buffa, J.A., Wang, Z., Gregory, J.C., Org, E., Wu, Y., Li, L., Smith, J.D., Tang, W.H.W., DiDonato, J.A., Lusis, A.J., Hazen, S.L., 2014. γ-Butyrobetaine Is a Proatherogenic Intermediate in Gut Microbial Metabolism of L-Carnitine to TMAO. Cell Metab. 20, 799–812. https://doi.org/10.1016/j.cmet.2014.10.006

Koeth, R.A., Wang, Z., Levison, B.S., Buffa, J.A., Org, E., Sheehy, B.T., Britt, E.B., Fu, X., Wu, Y., Li, L., Smith, J.D., DiDonato, J.A., Chen, J., Li, H., Wu, G.D., Lewis, J.D., Warrier, M., Brown, J.M., Krauss, R.M., Tang, W.H.W., Bushman, F.D., Lusis, A.J., Hazen, S.L., 2013. Intestinal microbiota metabolism of L-carnitine, a nutrient in red meat, promotes atherosclerosis. Nat. Med. 19, 576–585. https://doi.org/10.1038/nm.3145

Kwang, W.J., 2015. International Review of Cell and Molecular Biology, Academic Press. ed.

Lavalle, J.B., Yale, S.L., 2004. Cracking the Metabolic Code: The Nine Keys to Peak Health , Basic health Publications. ed.

Lavie, L., 2003. Obstructive sleep apnoea syndrome--an oxidative stress disorder. Sleep Med. Rev. 7, 35–51.

Lavie, L., Lavie, P., 2009. Molecular mechanisms of cardiovascular disease in OSAHS: the oxidative stress link. Eur. Respir. J. 33, 1467–1484. https://doi.org/10.1183/09031936.00086608

Lavie, L., Vishnevsky, A., Lavie, P., 2004. Evidence for lipid peroxidation in obstructive sleep apnea. Sleep 27, 123–128.

Lees, H.J., Swann, J.R., Wilson, I.D., Nicholson, J.K., Holmes, E., 2013. Hippurate: the natural history of a mammalian-microbial cometabolite. J. Proteome Res. 12, 1527–1546. https://doi.org/10.1021/pr300900b

Leung, C., Rivera, L., Furness, J.B., Angus, P.W., 2016. The role of the gut microbiota in NAFLD. Nat. Rev. Gastroenterol. Hepatol. 13, 412–425. https://doi.org/10.1038/nrgastro.2016.85

Li, P., Wu, J., Zhao, L., Feng, X., 2016. Effects and relationship of intermittent hypoxia on serum lipid levels, hepatic low-density lipoprotein receptor-related protein 1, and hypoxia-inducible factor 1α. Sleep Breath. 20, 167–173. https://doi.org/10.1007/s11325-015-1200-4

Lin, S.L., Zarrine-Afsar, A., Davidson, A.R., 2009. The osmolyte trimethylamine-N-oxide stabilizes the Fyn SH3 domain without altering the structure of its folding transition state. Protein Sci. Publ. Protein Soc. 18, 526–536. https://doi.org/10.1002/pro.52

Lindon, J.C., Nicholson, J.K., 2008. Spectroscopic and statistical techniques for information recovery in metabonomics and metabolomics. Annu. Rev. Anal. Chem. Palo Alto Calif 1, 45–69. https://doi.org/10.1146/annurev.anchem.1.031207.113026

Lindon, J.C., Nicholson, J.K., Holmes, E., Everett, J.R., 2000. Metabonomics: Metabolic processes studied by NMR spectroscopy of biofluids. Concepts Magn. Reson. 12, 289–320. https://doi.org/10.1002/1099-0534(2000)12:5<289::AID-CMR3>3.0.CO;2-W

Lupachyk, S., Watcho, P., Stavniichuk, R., Shevalye, H., Obrosova, I.G., 2013. Endoplasmic reticulum stress plays a key role in the pathogenesis of diabetic peripheral neuropathy. Diabetes 62, 944–952. https://doi.org/10.2337/db12-0716

Maes, C., Carmeliet, G., Schipani, E., 2012. Hypoxia-driven pathways in bone development, regeneration and disease. Nat. Rev. Rheumatol. 8, 358–366. https://doi.org/10.1038/nrrheum.2012.36

Mahadev, K., Wu, X., Zilbering, A., Zhu, L., Lawrence, J.T., Goldstein, B.J., 2001. Hydrogen peroxide generated during cellular insulin stimulation is integral to activation of the distal insulin signaling cascade in 3T3-L1 adipocytes. J. Biol. Chem. 276, 48662–48669. https://doi.org/10.1074/jbc.M105061200

Marin, J.M., Carrizo, S.J., Vicente, E., Agusti, A.G.N., 2005. Long-term cardiovascular outcomes in men with obstructive sleep apnoea-hypopnoea with or without treatment with continuous positive airway pressure: an observational study. Lancet Lond. Engl. 365, 1046–1053. https://doi.org/10.1016/S0140-6736(05)71141-7

Mason, J.B., Kodicek, E., 1970. The metabolism of niacytin in the rat. Trigonelline as a major metabolite of niacytin in the urine. Biochem. J. 120, 515–521.

Mason, S., Wadley, G.D., 2014. Skeletal muscle reactive oxygen species: a target of good cop/bad cop for exercise and disease. Redox Rep. Commun. Free Radic. Res. 19, 97–106. https://doi.org/10.1179/1351000213Y.0000000077

McGuire, M., Bradford, A., 1999. Chronic intermittent hypoxia increases haematocrit and causes right ventricular hypertrophy in the rat. Respir. Physiol. 117, 53–58.

McGuire, M., MacDermott, M., Bradford, A., 2002. Effects of chronic episodic hypoxia on rat upper airway muscle contractile properties and fiber-type distribution. Chest 122, 1012–1017.

Mesarwi, O.A., Shin, M.-K., Bevans-Fonti, S., Schlesinger, C., Shaw, J., Polotsky, V.Y., 2016. Hepatocyte Hypoxia Inducible Factor-1 Mediates the Development of Liver Fibrosis in a Mouse Model of Nonalcoholic Fatty Liver Disease. PloS One 11, e0168572. https://doi.org/10.1371/journal.pone.0168572

Miao, J., Ling, A.V., Manthena, P.V., Gearing, M.E., Graham, M.J., Crooke, R.M., Croce, K.J., Esquejo, R.M., Clish, C.B., Morbid Obesity Study Group, Vicent, D., Biddinger, S.B., 2015. Flavin-containing monooxygenase 3 as a potential player in diabetes-associated atherosclerosis. Nat. Commun. 6, 6498. https://doi.org/10.1038/ncomms7498

Mikami, T., Kita, K., Tomita, S., Qu, G.J., Tasaki, Y., Ito, A., 2000. Is allantoin in serum and urine a useful indicator of exercise-induced oxidative stress in humans? Free Radic. Res. 32, 235–244.

Minoguchi, K., Yokoe, T., Tanaka, A., Ohta, S., Hirano, T., Yoshino, G., O'Donnell, C.P., Adachi, M., 2006. Association between lipid peroxidation and inflammation in obstructive sleep apnoea. Eur. Respir. J. 28, 378–385. https://doi.org/10.1183/09031936.06.00084905

Montesi, S.B., Bajwa, E.K., Malhotra, A., 2012. Biomarkers of Sleep Apnea. Chest 142, 239–245. https://doi.org/10.1378/chest.11-2322

Moreno-Indias, I., Torres, M., Montserrat, J.M., Sanchez-Alcoholado, L., Cardona, F., Tinahones, F.J., Gozal, D., Poroyko, V.A., Navajas, D., Queipo-Ortuño, M.I., Farré, R., 2015. Intermittent hypoxia alters gut microbiota diversity in a mouse model of sleep apnoea. Eur. Respir. J. 45, 1055–1065. https://doi.org/10.1183/09031936.00184314

Nanduri, J., Peng, Y.-J., Yuan, G., Kumar, G.K., Prabhakar, N.R., 2015. Hypoxia-inducible factors and hypertension: lessons from sleep apnea syndrome. J. Mol. Med. Berl. Ger. 93, 473–480. https://doi.org/10.1007/s00109-015-1274-2

Nasser, S., Rees, P.J., 1992. Sleep apnoea: causes, consequences and treatment. Br. J. Clin. Pract. 46, 39–43.

Ndubuizu, O.I., Chavez, J.C., LaManna, J.C., 2009. Increased prolyl 4-hydroxylase expression and differential regulation of hypoxia-inducible factors in the aged rat brain. AJP Regul. Integr. Comp. Physiol. 297, R158–R165. https://doi.org/10.1152/ajpregu.90829.2008

Nicholson, J.K., Connelly, J., Lindon, J.C., Holmes, E., 2002. Metabonomics: a platform for studying drug toxicity and gene function. Nat. Rev. Drug Discov. 1, 153–161. https://doi.org/10.1038/nrd728

Nonaka, H., Tsujino, T., Watari, Y., Emoto, N., Yokoyama, M., 2001. Taurine prevents the decrease in expression and secretion of extracellular superoxide dismutase induced by homocysteine: amelioration of homocysteine-induced endoplasmic reticulum stress by taurine. Circulation 104, 1165–1170.

O'Halloran, K.D., McGuire, M., O'Hare, T., Bradford, A., 2002. Chronic intermittent asphyxia impairs rat upper airway muscle responses to acute hypoxia and asphyxia. Chest 122, 269–275.

Pang, D., 2014. Niacin and microvascular endothelial cell response to fatty acid excess and hypoxia. Western University.

Pastoris, O., Dossena, M., Foppa, P., Arnaboldi, R., Gorini, A., Villa, R.F., Benzi, G., 1995. Modifications by chronic intermittent hypoxia and drug treatment on skeletal muscle metabolism. Neurochem. Res. 20, 143–150.

Pialoux, V., Mounier, R., Brown, A.D., Steinback, C.D., Rawling, J.M., Poulin, M.J., 2009. Relationship between oxidative stress and HIF-1α mRNA during sustained hypoxia in humans. Free Radic. Biol. Med. 46, 321–326. https://doi.org/10.1016/j.freeradbiomed.2008.10.047

Polak, J., Shimoda, L.A., Drager, L.F., Undem, C., McHugh, H., Polotsky, V.Y., Punjabi, N.M., 2013. Intermittent Hypoxia Impairs Glucose Homeostasis in C57BL6/J Mice: Partial Improvement with Cessation of the Exposure. SLEEP. https://doi.org/10.5665/sleep.3040

Polotsky, V.Y., Li, J., Punjabi, N.M., Rubin, A.E., Smith, P.L., Schwartz, A.R., O'Donnell, C.P., 2003. Intermittent hypoxia increases insulin resistance in genetically obese mice. J. Physiol. 552, 253–264. https://doi.org/10.1113/jphysiol.2003.048173

Poroyko, V.A., Carreras, A., Khalyfa, A., Khalyfa, A.A., Leone, V., Peris, E., Almendros, I., Gileles-Hillel, A., Qiao, Z., Hubert, N., Farré, R., Chang, E.B., Gozal, D., 2016. Chronic Sleep Disruption Alters Gut Microbiota, Induces Systemic and Adipose Tissue Inflammation and Insulin Resistance in Mice. Sci. Rep. 6, 35405. https://doi.org/10.1038/srep35405

Pullinger, C.R., Eng, C., Salen, G., Shefer, S., Batta, A.K., Erickson, S.K., Verhagen, A., Rivera, C.R., Mulvihill, S.J., Malloy, M.J., Kane, J.P., 2002. Human cholesterol 7α-hydroxylase (CYP7A1) deficiency has a hypercholesterolemic phenotype. J. Clin. Invest. 110, 109–117. https://doi.org/10.1172/JCI15387

Rafacho, A., Gonçalves-Neto, L.M., Ferreira, F.B.D., Protzek, A.O.P., Boschero, A.C., Nunes, E.A., Zoccal, D.B., 2013. Glucose homoeostasis in rats exposed to acute intermittent hypoxia. Acta Physiol. Oxf. Engl. 209, 77–89. https://doi.org/10.1111/apha.12118

Randrianarisoa, E., Lehn-Stefan, A., Wang, X., Hoene, M., Peter, A., Heinzmann, S.S., Zhao, X., Königsrainer, I., Königsrainer, A., Balletshofer, B., Machann, J., Schick, F., Fritsche, A., Häring, H.-U., Xu, G., Lehmann, R., Stefan, N., 2016. Relationship of Serum Trimethylamine N-Oxide (TMAO) Levels with early Atherosclerosis in Humans. Sci. Rep. 6, 26745. https://doi.org/10.1038/srep26745

Robinson, F.A., 2013. The Vitamin Co-Factors of Enzyme Systems, Elsevier. ed.

Sacramento, J.F., Ribeiro, M.J., Rodrigues, T., Guarino, M.P., Diogo, L.N., Seiça, R., Monteiro, E.C., Matafome, P., Conde, S.V., 2016. Insulin resistance is associated with tissue-specific regulation of HIF-1α and HIF-2α during mild chronic intermittent hypoxia. Respir. Physiol. Neurobiol. 228, 30–38. https://doi.org/10.1016/j.resp.2016.03.007

Sánchez-de-la-Torre, M., Campos-Rodriguez, F., Barbé, F., 2013. Obstructive sleep apnoea and cardiovascular disease. Lancet Respir. Med. 1, 61–72. https://doi.org/10.1016/S2213-2600(12)70051-6

Sauve, A.A., 2007. NAD+ and Vitamin B3: From Metabolism to Therapies. J. Pharmacol. Exp. Ther. 324, 883–893. https://doi.org/10.1124/jpet.107.120758

Schaffer, S.W., Jong, C.J., Ramila, K.C., Azuma, J., 2010. Physiological roles of taurine in heart and muscle. J. Biomed. Sci. 17 Suppl 1, S2. https://doi.org/10.1186/1423-0127-17-S1-S2

Schugar, R.C., Brown, J.M., 2015. Emerging roles of flavin monooxygenase 3 in cholesterol metabolism and atherosclerosis. Curr. Opin. Lipidol. 26, 426–431. https://doi.org/10.1097/MOL.0000000000000215

Schuller-Levis, G.B., Park, E., 2003. Taurine: new implications for an old amino acid. FEMS Microbiol. Lett. 226, 195–202.

Serkova, N., Fuller, T.F., Klawitter, J., Freise, C.E., Niemann, C.U., 2005. H-NMR-based metabolic signatures of mild and severe ischemia/reperfusion injury in rat kidney transplants. Kidney Int. 67, 1142–1151. https://doi.org/10.1111/j.1523-1755.2005.00181.x

Shen, L., Sun, X., Fu, Z., Yang, G., Li, J., Yao, L., 2012. The fundamental role of the p53 pathway in tumor metabolism and its implication in tumor therapy. Clin. Cancer Res. Off. J. Am. Assoc. Cancer Res. 18, 1561–1567. https://doi.org/10.1158/1078-0432.CCR-11-3040

Shih, D.M., Wang, Z., Lee, R., Meng, Y., Che, N., Charugundla, S., Qi, H., Wu, J., Pan, C., Brown, J.M., Vallim, T., Bennett, B.J., Graham, M., Hazen, S.L., Lusis, A.J., 2015. Flavin containing monooxygenase 3 exerts broad effects on glucose and lipid metabolism and atherosclerosis. J. Lipid Res. 56, 22–37. https://doi.org/10.1194/jlr.M051680

Shockcor, J.P., Holmes, E., 2002. Metabonomic applications in toxicity screening and disease diagnosis. Curr. Top. Med. Chem. 2, 35–51.

Shortt, C.M., Fredsted, A., Chow, H.B., Williams, R., Skelly, J.R., Edge, D., Bradford, A., O'Halloran, K.D., 2014. Reactive oxygen species mediated diaphragm fatigue in a rat model of chronic intermittent hypoxia. Exp. Physiol. 99, 688–700. https://doi.org/10.1113/expphysiol.2013.076828

Skelly, J.R., Edge, D., Shortt, C.M., Jones, J.F.X., Bradford, A., O'Halloran, K.D., 2012. Tempol ameliorates pharyngeal dilator muscle dysfunction in a rodent model of chronic intermittent hypoxia. Am. J. Respir. Cell Mol. Biol. 46, 139–148. https://doi.org/10.1165/rcmb.2011-0084OC

Somers, V.K., White, D.P., Amin, R., Abraham, W.T., Costa, F., Culebras, A., Daniels, S., Floras, J.S., Hunt, C.E., Olson, L.J., Pickering, T.G., Russell, R., Woo, M., Young, T., American Heart Association Council for High Blood Pressure Research Professional Education Committee, Council on Clinical Cardiology, American Heart Association Stroke Council, American Heart Association Council on Cardiovascular Nursing, American College of Cardiology Foundation, 2008. Sleep apnea and cardiovascular disease: an American Heart Association/american College Of Cardiology Foundation Scientific Statement from the American Heart Association Council for High Blood Pressure Research Professional Education Committee, Council on Clinical Cardiology, Stroke Council, and Council On Cardiovascular Nursing. In collaboration with the National Heart, Lung, and Blood Institute National Center on Sleep Disorders Research (National Institutes of Health). Circulation 118, 1080–1111. https://doi.org/10.1161/CIRCULATIONAHA.107.189375

Stroka, D.M., Burkhardt, T., Desbaillets, I., Wenger, R.H., Neil, D.A., Bauer, C., Gassmann, M., Candinas, D., 2001. HIF-1 is expressed in normoxic tissue and displays an organ-specific regulation under systemic hypoxia. FASEB J. Off. Publ. Fed. Am. Soc. Exp. Biol. 15, 2445–2453. https://doi.org/10.1096/fj.01-0125com

Sun, X., Jiao, X., Ma, Y., Liu, Y., Zhang, L., He, Y., Chen, Y., 2016. Trimethylamine N-oxide induces inflammation and endothelial dysfunction in human umbilical vein endothelial cells via activating ROS-TXNIP-NLRP3 inflammasome. Biochem. Biophys. Res. Commun. 481, 63–70. https://doi.org/10.1016/j.bbrc.2016.11.017

Teft, W.A., Morse, B.L., Leake, B.F., Wilson, A., Mansell, S.E., Hegele, R.A., Ho, R.H., Kim, R.B., 2017. Identification and Characterization of Trimethylamine-N-oxide Uptake and Efflux Transporters. Mol. Pharm. 14, 310–318. https://doi.org/10.1021/acs.molpharmaceut.6b00937

Thornton, J.D., Chandriani, K., Thornton, J.G., Farooq, S., Moallem, M., Krishnan, V., Auckley, D., 2010. Assessing the Prioritization of Primary Care Referrals for Polysomnograms. Sleep 33, 1255–1260.

Tiganis, T., 2011. Reactive oxygen species and insulin resistance: the good, the bad and the ugly. Trends Pharmacol. Sci. 32, 82–89. https://doi.org/10.1016/j.tips.2010.11.006

Tkachev, V.O., Menshchikova, E.B., Zenkov, N.K., 2011. Mechanism of the Nrf2/Keap1/ARE signaling system. Biochem. Biokhimiia 76, 407–422.

Toffoli, S., Feron, O., Raes, M., Michiels, C., 2007. Intermittent hypoxia changes HIF-1alpha phosphorylation pattern in endothelial cells: unravelling of a new PKA-dependent regulation of HIF-1alpha. Biochim. Biophys. Acta 1773, 1558–1571. https://doi.org/10.1016/j.bbamcr.2007.06.002

Ufnal, M., Zadlo, A., Ostaszewski, R., 2015. TMAO: A small molecule of great expectations. Nutrition 31, 1317–1323. https://doi.org/10.1016/j.nut.2015.05.006

Van Thienen, R., Masschelein, E., D'Hulst, G., Thomis, M., Hespel, P., 2017. Twin Resemblance in Muscle HIF-1α Responses to Hypoxia and Exercise. Front. Physiol. 7. https://doi.org/10.3389/fphys.2016.00676

Vanuxem, D., Badier, M., Guillot, C., Delpierre, S., Jahjah, F., Vanuxem, P., 1997. Impairment of muscle energy metabolism in patients with sleep apnoea syndrome. Respir. Med. 91, 551–557.

Wang, X., Yu, Q., Yue, H., Zeng, S., Cui, F., 2015. Effect of Intermittent Hypoxia and Rimonabant on Glucose Metabolism in Rats: Involvement of Expression of GLUT4 in Skeletal Muscle. Med. Sci. Monit. Int. Med. J. Exp. Clin. Res. 21, 3252–3260.

Wang, Z., Klipfell, E., Bennett, B.J., Koeth, R., Levison, B.S., Dugar, B., Feldstein, A.E., Britt, E.B., Fu, X., Chung, Y.-M., Wu, Y., Schauer, P., Smith, J.D., Allayee, H., Tang, W.H.W., DiDonato, J.A., Lusis, A.J., Hazen, S.L., 2011. Gut flora metabolism of phosphatidylcholine promotes cardiovascular disease. Nature 472, 57–63. https://doi.org/10.1038/nature09922

Warrier, M., Shih, D.M., Burrows, A.C., Ferguson, D., Gromovsky, A.D., Brown, A.L., Marshall, S., McDaniel, A., Schugar, R.C., Wang, Z., Sacks, J., Rong, X., Vallim, T. de A., Chou, J., Ivanova, P.T., Myers, D.S., Brown, H.A., Lee, R.G., Crooke, R.M., Graham, M.J., Liu, X., Parini, P., Tontonoz, P., Lusis, A.J., Hazen, S.L., Temel, R.E., Brown, J.M., 2015. The TMAO-Generating Enzyme Flavin Monooxygenase 3 Is a Central Regulator of Cholesterol Balance. Cell Rep. https://doi.org/10.1016/j.celrep.2014.12.036

Williams, A.L., Chen, L., Scharf, S.M., 2010. Effects of allopurinol on cardiac function and oxidant stress in chronic intermittent hypoxia. Sleep Breath. Schlaf Atm. 14, 51–57. https://doi.org/10.1007/s11325-009-0279-x

Williams, H.R.T., Cox, I.J., Walker, D.G., Cobbold, J.F.L., Taylor-Robinson, S.D., Marshall, S.E., Orchard, T.R., 2010. Differences in gut microbial metabolism are responsible for reduced hippurate synthesis in Crohn's disease. BMC Gastroenterol. 10, 108. https://doi.org/10.1186/1471-230X-10-108

Xu, H., Zheng, X., Qian, Y., Guan, J., Yi, H., Zou, J., Wang, Y., Meng, L., Zhao, A., Yin, S., Jia, W., 2016. Metabolomics Profiling for Obstructive Sleep Apnea and Simple Snorers. Sci. Rep. 6, 30958. https://doi.org/10.1038/srep30958

Yamauchi, M., Nakano, H., Maekawa, J., Okamoto, Y., Ohnishi, Y., Suzuki, T., Kimura, H., 2005. Oxidative stress in obstructive sleep apnea. Chest 127, 1674–1679. https://doi.org/10.1378/chest.127.5.1674

Yeung, S.J., Pan, J., Lee, M.-H., 2008. Roles of p53, MYC and HIF-1 in regulating glycolysis - the seventh hallmark of cancer. Cell. Mol. Life Sci. CMLS 65, 3981–3999. https://doi.org/10.1007/s00018-008-8224-x

Yildirim, Z., Kilic, N., Ozer, C., Babul, A., Take, G., Erdogan, D., 2007. Effects of Taurine in Cellular Responses to Oxidative Stress in Young and Middle-Aged Rat Liver. Ann. N. Y. Acad. Sci. 1100, 553–561. https://doi.org/10.1196/annals.1395.061

Yuan, G., Nanduri, J., Bhasker, C.R., Semenza, G.L., Prabhakar, N.R., 2005. Ca2+/calmodulin kinase-dependent activation of hypoxia inducible factor 1 transcriptional activity in cells subjected to intermittent hypoxia. J. Biol. Chem. 280, 4321–4328. https://doi.org/10.1074/jbc.M407706200

Yuan, G., Nanduri, J., Khan, S., Semenza, G.L., Prabhakar, N.R., 2008. Induction of HIF-1alpha expression by intermittent hypoxia: involvement of NADPH oxidase, Ca2+ signaling, prolyl hydroxylases, and mTOR. J. Cell. Physiol. 217, 674–685. https://doi.org/10.1002/jcp.21537

Ząbek, A., Stanimirova, I., Deja, S., Barg, W., Kowal, A., Korzeniewska, A., Orczyk-Pawiłowicz, M., Baranowski, D., Gdaniec, Z., Jankowska, R., Młynarz, P., 2015. Fusion of the (1)H NMR data of serum, urine and exhaled breath condensate in order to discriminate chronic obstructive pulmonary disease and obstructive sleep apnea syndrome. Metabolomics Off. J. Metabolomic Soc. 11, 1563–1574. https://doi.org/10.1007/s11306-015-0808-5

Zaugg, K., Yao, Y., Reilly, P.T., Kannan, K., Kiarash, R., Mason, J., Huang, P., Sawyer, S.K., Fuerth, B., Faubert, B., Kalliomäki, T., Elia, A., Luo, X., Nadeem, V., Bungard, D., Yalavarthi, S., Growney, J.D., Wakeham, A., Moolani, Y., Silvester, J., Ten, A.Y., Bakker, W., Tsuchihara, K., Berger, S.L., Hill, R.P., Jones, R.G., Tsao, M., Robinson, M.O., Thompson, C.B., Pan, G., Mak, T.W., 2011. Carnitine palmitoyltransferase 1C promotes cell survival and tumor growth under conditions of metabolic stress. Genes Dev. 25, 1041–1051. https://doi.org/10.1101/gad.1987211

Zeisel, S.H., Gettner, S., Youssef, M., 1989. Formation of aliphatic amine precursors of N-nitrosodimethylamine after oral administration of choline and choline analogues in the rat. Food Chem. Toxicol. Int. J. Publ. Br. Ind. Biol. Res. Assoc. 27, 31–34.

Zhang, L.S., Davies, S.S., 2016. Microbial metabolism of dietary components to bioactive metabolites: opportunities for new therapeutic interventions. Genome Med. 8. https://doi.org/10.1186/s13073-016-0296-x

Zhu, Y., Prives, C., 2009. p53 and Metabolism: The GAMT Connection. Mol. Cell 36, 351–352. https://doi.org/10.1016/j.molcel.2009.10.026

Figures

Figure A: Study design timeline.
Mice were exposed to cycles of 30 s to the FIO2 of 6% - 30 s to the FIO2 of 21%. These cycles were repeated 8h/day (white square) interspersed by 16h normoxia (black square) for 35 days. **1.** Haematocrit measurements were performed at different time-points (1, 3, 8, 14, 21, 28, 35 days, n = 7 per time point), directly after the 8h of exposure to IH or normoxia (white square). **2.** Glucose tolerance tests were conducted at different time-points (days 0, 1, 3, 7, 14, 21, 28, 34, n =10 for sham and n = 11 for ChIH per time point) directly after the 8h of exposure to IH or normoxia (white square). **3. Urine collection for metabonomic analysis.** To realize metabonomic analyses, another group of animals were placed at days 0, 1, 3, 7, 14, 21, 28 and 34, directly after the 8h of exposure to IH or normoxia (white square), in metabolic cage during 16h normoxia (black square) and urines collected (n=7 for each group and time-point). Biochemical pathways potentially involved in metabonomic changes were then verified: HIF1α (hypoxia inducible factor 1α) nuclear abundance at days 1 (ChIH n=12, Sham n=10) and 35 (ChIH n=8, Sham n=9) and GAMT (GuanidinoAcetate MethylTransferase) abundance at day 35 (ChIH n=11 , Sham n =10).

Figure B: Metabonomic alteration induced during ChIH in mice. 1. PLS-DA (scores plot) of ^{1}H NMR spectra of urine samples collected over a 16h-period after 0, 1, 2, 3, 4, 7, 14, 21, 28 and 34 days of ChIH (black squares, n = 7 per time point) and normoxia (green squares, n = 7 per time point). The model parameters were: $R^2Xcum = 0.377$; $R^2Ycum = 0.461$; $Q^2cum = 0.366$; and Hotelling's T2 : 0.95. *p = 5.58 x 10-9, CV ANOVA test. **2.** Cross-validation plot with a permutation test repeated 50 times. The permuted R^2 (in green) and Q^2 (in blue) values located in the left side of the graph were lower than the original points to the right and Q^2 regression lines (in blue) have negative intercepts (Y axis intercepts : $R^2 = (0.0, 0.129)$; and $Q^2 = (0.0, -0.185)$) indicate the validity of our PLS-DA model.

Figure C: Representative 500 MHz ^{1}HNMR urine spectra from sham and ChIH animals. a – creatine; b – citrate ; c – methylamine ; d – dimethylamine ; e – tryptophan ; f – carnitine ; g – sarcosine ; h – glycine ; i – choline ; j – trans-aconitate ; k – creatinine ; Trimethylamine (TMA); trimethylamine N oxide (TMAO).

Figure D: Evolution of metabonomic alteration induced during ChIH exposition.
A. PLS-DA (scores plot) of ^{1}H-NMR spectra of urine samples collected over a 16h-period after 0,1,2,3,4 days (early event, red squares, n = 7 per time point) and 7, 14, 21, 28, 34 days (chronic alteration, blue squares, n = 7 per time point) of ChIH. The model parameters were: $R^2Xcum = 0.434$; $R^2Ycum = 0.69$; $Q^2cum = 0.486$; and Hotelling's T2 : 0.95. *p = 9.07 x10-6, CV ANOVA test. **B.** Cross-validation plot (R^2 in green, Q^2 in blue with a permutation test repeated 50 times. The permuted R^2 (in green) and Q^2 (in blue) values located in the left side of the graph were lower than the original points to the right and Q^2 regression lines (in blue) have negative intercepts (Y axis intercepts : $R^2 = (0.0, 0.188)$; and $Q^2 = (0.0, -0.201)$) indicate the validity of our PLS-DA model.

Figure E: Effect of ChIH on HIF1α nuclear abundance in liver.
1. Representation blot of HIF1 activation after a ChIH exposure.
HIF1α protein abundance in the liver after 1 day of ChIH. The positive control corresponds to nuclear extract of Raw cells exposed to continuous hypoxia during 24h. **2. HIF1α nuclear abundance in liver.** HIF1α nuclear abundance in the liver after 1 day of normoxia (n = 10) or ChIH (n = 12) and 35 days of normoxia (n = 9) or ChIH (n = 8). Median, percentile 25 and 75%, *p< 0.01 between ChIH, *p<0.01 sham vs ChIH, ANOVA on ranks.

Figure F: Effect of ChIH on haematocrit.
Haematocrit measurement performed at different time points (1, 3, 8, 14, 21, 28, 35 days) directly after the 8h of exposure to IH (n = 7 per time point) or normoxia (n = 7 per time point excepted days 14 and 28). Mean ± sem * p< 0.001 One way ANOVA.

Figure G: Evolution of ChIH effect on glycemia. Blood glucose area under the curve (AUC glycemia) during a glucose tolerance test (D-Glucose 2g/kg b.w. over 120 min) performed at different time points (before and at day 1, 3, 7, 14, 21, 28 and 34) directly after the exposure to ChIH (in grey, n = 10 per time point) or normoxia (in black, n = 9 per time point). Median, percentile 25 and 75%, *p<0.001 between ChIH, *p<0.001 sham vs ChIH, ANOVA on ranks.

Figure H: GAMT protein abundance after 35 days of ChIH. 1. Total GAMT protein abundance in liver. p = 0.443, Student's unpaired t-test. **2. Proportions of GAMT forms.** *p <0.05, Chi square. **3. Densitometric analysis of total GAMT protein abundance.** Representative blot realized using reducing PAGE SDS followed by a Western Blot. RPLP0 was used as loading control. **4. Densitometric analysis of GAMT forms proportions.** Representative blot realized using non-reducing PAGE SDS followed by a Western Blot.

Figure I: Schematic representation of metabolic modifications induced by ChIH exposure.
Red arrow indicates a metabolite decrease and green arrow a metabolite increase in urine sample of ChIH. Chronic intermittent hypoxia (ChIH), xanthine oxidase (XO), reactive oxygen species (ROS), hypoxia inducible factor 1 (HIF1), lactate dehydrogenase (LDH), pyruvate dehydrogenase kinase 1 (PDK1), pyruvate dehydrogenase (PDH) acetylCoA (AcCoA), trimethylamine (TMA), dimethylamine (DMA), methylamine (MA), trimethylamine N oxide (TMAO), cardiovascular (CV), methionine (Met.), glycine (Gly.), sarcosine (Sarc.), guanidinoacetate (Guanido.), guanidinoacetate methyltransferase (GAMT).

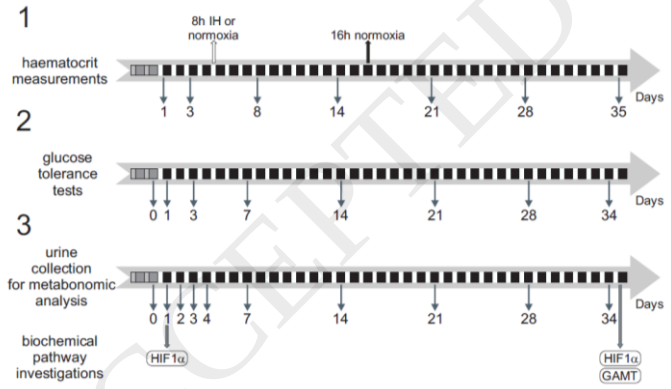

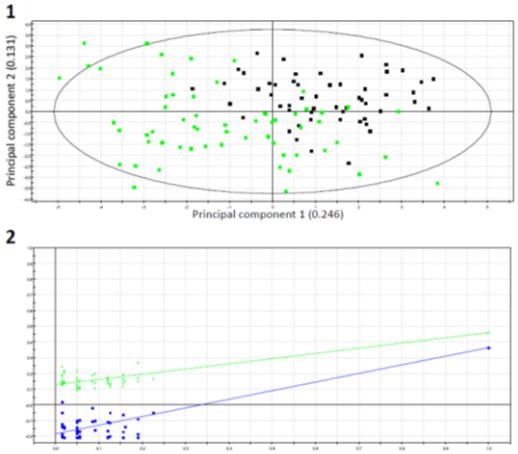

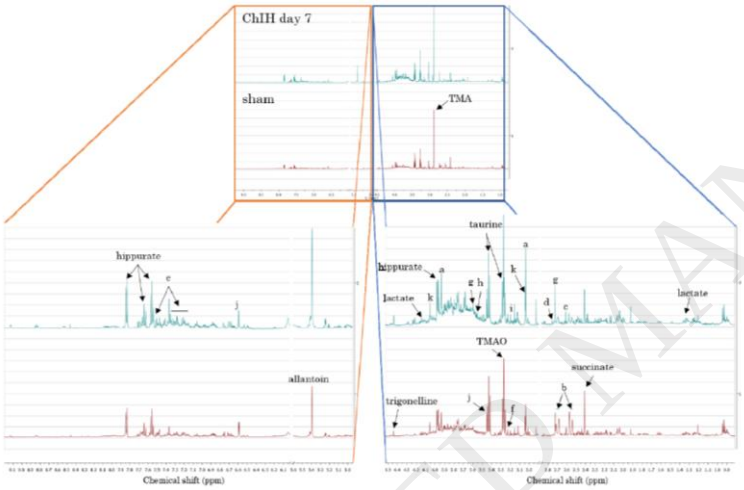

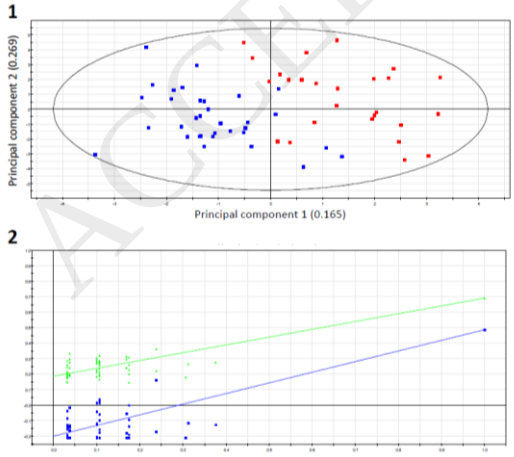

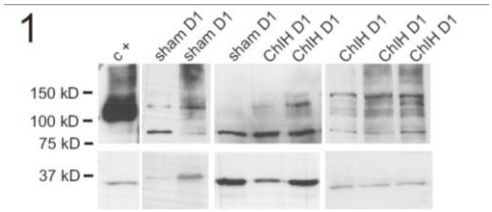

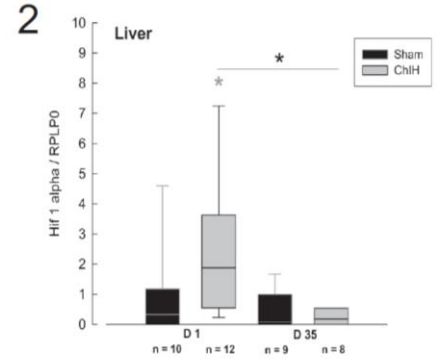

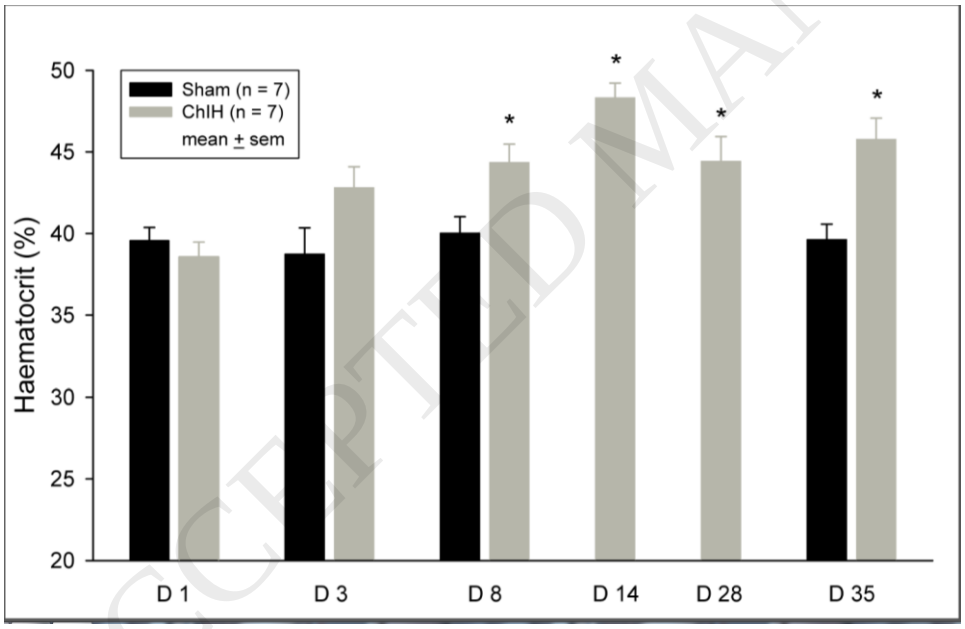

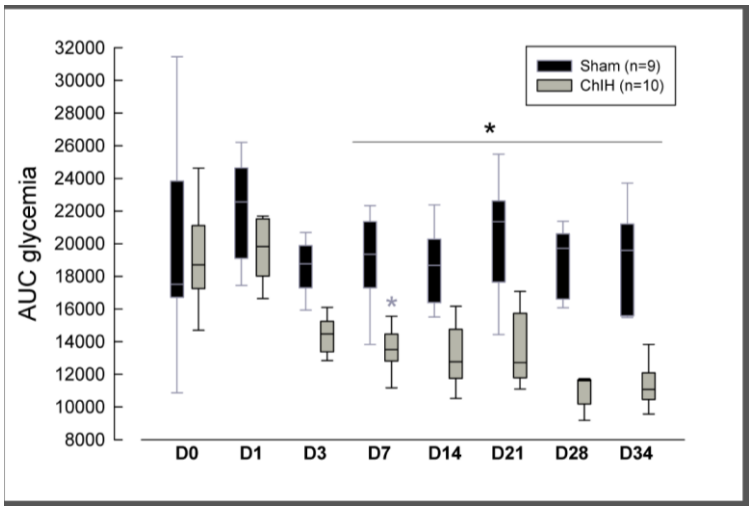

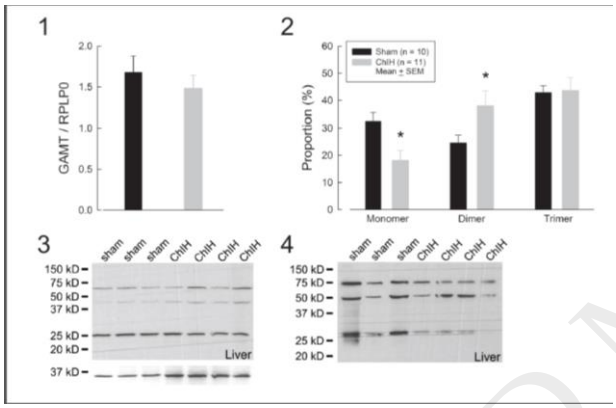

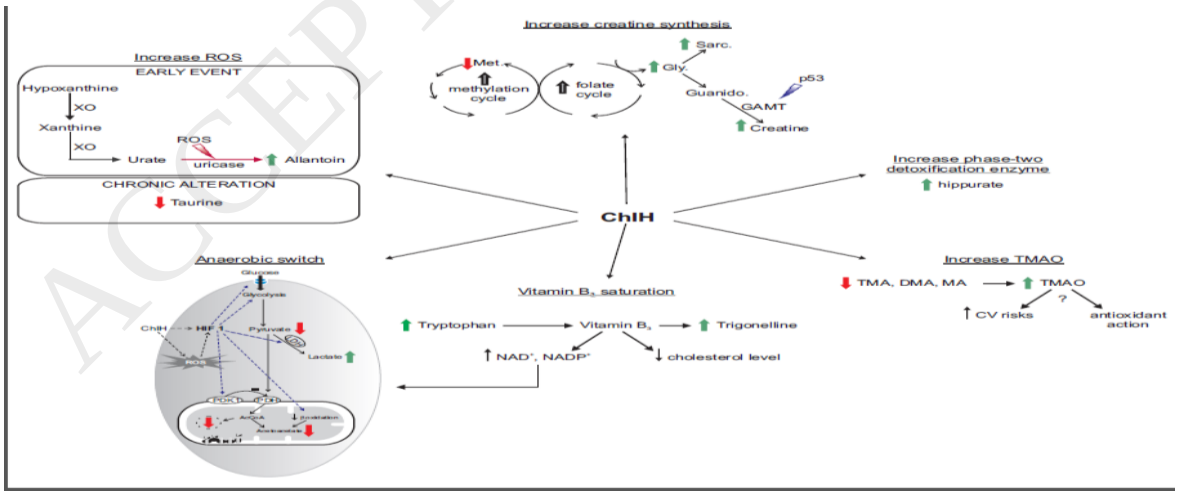

Appendices

Appendix A : Evolution of ChIH effect on body weight and food intake. 1. Body Weight evolution. Mean ± sem, NS (p = 0.121), Two way Repeated Measures ANOVA. **2. Food intake evolution.** Mean ± sem, NS, Two way Repeated Measures ANOVA (p = 0.397).

Appendix B : Variable Important in projection (VIP) of spectral sub-region after a ChIH exposition. Plot of different spectral sub-region whose concentration were modified and screening a VIP > 0.7 follow a ChIH exposition compared to normoxic condition.

Appendix C : Variable Important in projection (VIP) of spectral sub-region during an exposure of chronic intermittent hypoxia (ChIH). Plot of different spectral sub-region whose concentration were modified over the hypoxic condition and screening a VIP > 0.7.

Appendix D: Analysis of GAMT forms using non-reducing conditions and reducing SDS-PAGE on liver extracts from sham mice. Representative blot. Ponceau Red was used as loading control.

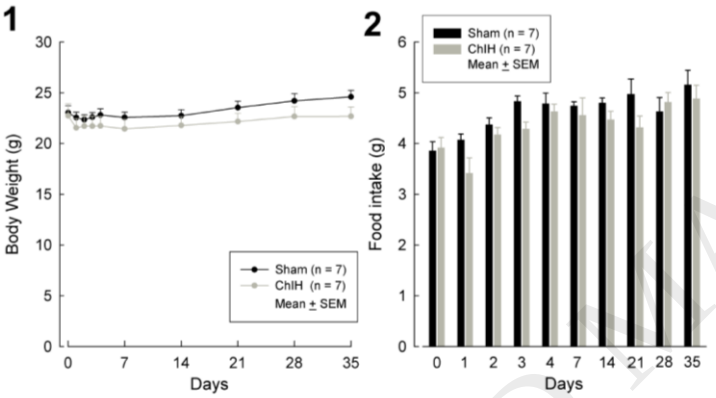

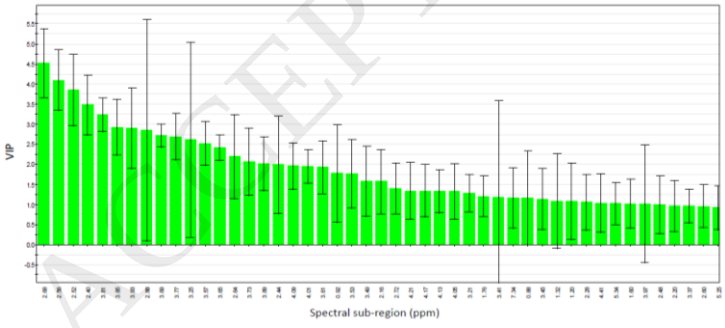

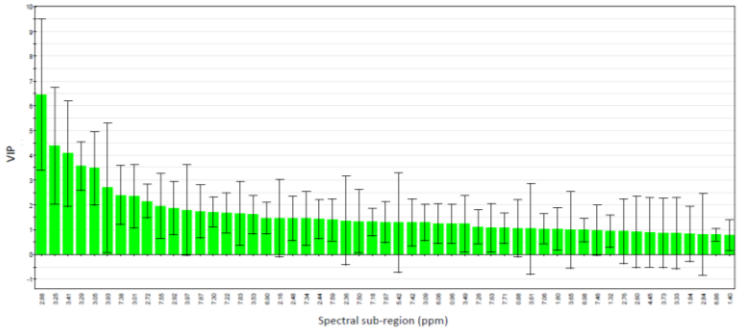

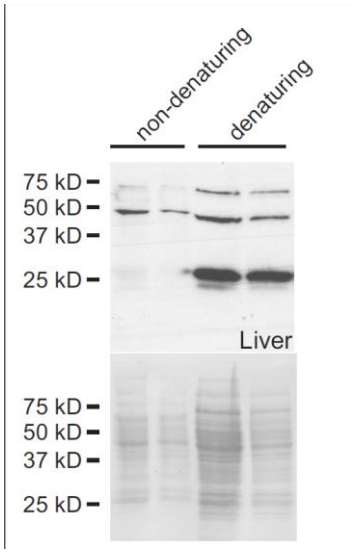

Tables

Table A : List of metabolites with changes in urine concentration in ChIH as compared to sham urines. Identification of spectral sub-region screening a VIP (Variable important in projection) values >0.7. Singlet (s), doublet (d), triplet (t), multiplet (m), quadruplet (q).

Increase			Decrease		
Identification	Chemical shift	VIP	Identification	Chemical shift	VIP
Lactate	1.32 (d)	1.08	Isoleucine/ Leucine	0.88 to 0.92 (m)	1.77
Trimethylamine N oxide	3.21 (s)	1.29	Isoleucine	1.20 (m)	1.08
Trans-aconitate	3.45 (s)	1.14	Methionine	2.16 (s)	1.57
Glycine	3.53 (s)	1.76	Acetoacetate	2.28 (s)	1.05
Sarcosine	3.61 (s)	1.93	Pyruvate	2.36 (s)	0.87
Creatine	3.93 (s)	2.90	Succinate	2.4 to 2.44 (s)	3.48
Hippurate	3.97 (d)	1.01	N acetylaspartate	2.52 (q)	3.86
Creatinine	4.05 (s)	1.32	Methylamine	2.56 to 2.60 (s)	4.10
Lactate	4.13 to 4.17 (q)	1.34	Citrate	2.68 (d)	4.52
Trigonelline	4.41	1.03	Dimethylamine	2.72 (s)	1.39
Allantoin	5.34 (s)	1.02	Trimethylamine	2.88 (s)	2.85
Hippurate	7.79 (d)	0.77	Taurine	3.25 (t)	2.61
			Taurine	3.41 (t)	1.18

Table B : List of metabolites with changes in urine concentration in chronic alteration of ChIH as compared to early event. Identification of spectral sub-region screening a VIP (Variable important in projection) values >0.7. Singlet (s), doublet (d), triplet (t), multiplet (m), quadruplet (q).

Increase			Decrease		
Identification	Chemical shift	VIP	Identification	Chemical shift	VIP
Methylamine	2.60 (s)	0.92	Isoleucine/ Leucine	0.88 (m)	0.98
Dimethylamine	2.72 (s)	2.05	Methionine	2.16 (s)	1.67
Trimethylamine	2.84 to 2.88 (s)	5.93	Acetoacetate	2.28 (s)	0.78
Glycine	3.53 (s)	1.73	Succinate	2.4 to 2.44 (s)	1.35
Hippurate	3.97 (d)	1.76	N acetylaspartate	2.52 (q)	0.91
Tryptophan	7.18 (t)	1.19	Citrate	2.68 (d)	1.49
Tryptophan	7.26 to 7.30 (q)	1.61	Creatine / creatinine	3.01 to 3.05 (s)	3.20
Tryptophan	7.50 (d)	1.25	Cis-aconitate	3.09 (d)	1.18
Hippurate	7.55 and 7.59 (d)	1.82	Choline / carnitine	3.17 (s)	0.78
Hippurate	7.63 (t)	1	Taurine	3.25 (t)	4.12
Tryptophan	7.71 (d)	1.07	Taurine	3.41 (t)	3.96
Hippurate	7.83 to 7.87 (d)	1.65	Trans-aconitate	3.45 (s)	1.19
			Sarcosine	3.61 (s)	0.96
			N,n-Dimethylglycine	3.73	1.21
			Creatine	3.93 (s)	2.67
			Allantoin	5.42 (s)	1.21